Electron-Acoustic Waves with Orbital Angular Momentum

By

Khurram Shahzad

Department of Physics

Quaid-i-Azam University

Islamabad, Pakistan.

2013

Certificate

This is to certify that Mr. Khurram Shahzad has carried out the theoretical work contained in this dissertation under my supervision and is accepted in its present form by the Department of Physics, Quaid-i-Azam University Islamabad as certifying the dissertation requirement for the degree of Master of Philosophy in Physics.

Submitted through

Chairman

Zaka-ullah

Prof. Dr. Muhammad Zakaullah

Department of Physics

Quaid-i-Azam university

Islamabad, Pakistan.

Supervisor

Dr. Shahid Ali

Assistant Professor

National Centre for Physics

QAU Campus Islamabad,

Pakistan.

This thesis is dedicated to my loving parents and to my friends.

Contents

List of Figures

ACKNOWLEDGEMENTS

I owe my profoundest thanks to Allah Almighty, the most benevolent and merciful, Who created the universe with the ideas of beauty, symmetry and harmony, as well as gave us the abilities to discover the universe. I offer my humblest thanks to the Prophet Muhammad (peace be upon him), who is forever the source of guidance and knowledge for humanity.

First and foremost, my utmost gratitude goes to Dr. Shahid Ali, Assistant Professor at National Centre for Physics (NCP), who is my research supervisor. From the formative stages, to the final draft, I owe immense debt of gratitude to my supervisor for his invaluable guidance and support. Friendly discussion with him has always stimulated my mind and gave me insight of research. I will never forget his sincerity and encouragement for research.

I am thankful to Dr. Hamid Saleem, DG (NCP) for his kind concern and consideration regarding my studies at NCP.

I am also grateful to the Chairman, Department of Physics, for providing me moral support and the permission to work at NCP. Very special thanks are due to Prof. P. K. Shukla, Ruhr University, and Dr. Arshad Majeed Mirza for useful discussions. My immense gratitude goes to all the teachers of Physics Department as well.

My heartiest thanks to all members of Plasma Physics Group, at NCP, which includes of Dr. Shabbir, Sadeeq, Abdul Rahman, Ishtiaq, Miss. Nazia, Miss. Ammara, my class fellows, Atif, Babar Ali, Asid Ali, Kashif and my all other university fellows who helped me one-way or the other.

Special thanks to my good friends, Imran, Shoaib, Mushtaq and my cousins who encouraged me a lot for research.

My sincere thanks to my loving parents, uncles, nice sisters, kind brothers for unconditional love, guidance, and support.

(Khurram Shahzad)

Abstract

The electron-acouetic (EA) waves carrying orbital angular momentum are investigated in a collisionless, unmagnetized uniform plasma. The latter is basically a two-temperature electron plasma composed of two populations of electrons, e.g. the inertial cold electrons and the Boltzmann distributed hot electrons with a neutralizing background of static ions. By employing the fluid equations, the dispersion relation for the EA waves is solved for a beam type solution under the paraxial approximation and also discussed the Laguerre-Gaussian (LG) solutions. An approximate solution for the electrostatic potential problem is obtained and the electric field components are now expressed in terms of LG potential representing the field lines as helical structures. Furthermore, the energy flux and orbital angular momentum states carried by the EA beam are studied in terms of LG potential perturbations. Numerically, it is revealed that the radial and angular mode indices strongly modify the profiles of the LG potential. The present results are important in the context of trapping and transporting the plasma particles and energy by the EA beams involving the orbital angular momentum states in laser produced plasma as well as in space plasmas, where two distinct populations of electrons exist.

Chapter 1

Introduction to Plasma

The electromagnetic forces are very important in the structure formation for example the stable atoms, molecules, and crystalline solids. It is well-known that there are three states of matter, such as the solid, liquid, and gas. In general, any one of these states can be converted into other through the exchange of energy. Water molecule H_2O is a remarkable example, which is found in all these states. Obviously, when energy is supplied to matter in its solid form, it decomposes and the solid will be converted into liquid and then liquid into gaseous state, by further increasing the energy up to atomic ionization state. Due to thermal decomposition, the interatomic bonds break before ionizing, which decomposing the matter into ions and electrons. These oppositely charged particles exhibit a collective behavior and such an assemblage is called plasma. On the other hand, in the reverse process the energy is extracted out from the matter. The degree of ionization of a plasma is defined as, " the ratio between the number of ionized atoms and the total number of atoms in a unit volume," showing that the plasma is ionized completely, strongly or weakly. When a gas is ionized, the new forces arise in the plasma between the plasma particles and the dynamical behavior is influenced by the external electric and magnetic fields.

In the earlier age of the Universe, it was assumed that everything was plasma. In fact, it is thought that almost 99% of our Universe exists in the state of plasma. All the stars, nebulae, including sun are composed of an ionized gas. Thus, solar winds coming from the sun, consist of charged particles as streams. The Earth is totally covered with charged particles that are trapped in the magnetic field of the Earth. Besides, interstellar spaces, are also filled with

plasma. However, it is not very difficult to find the plasma on the Earth. Liquid and solid systems can be considered sometime to express collective electromagnetic effects describing the ionized gas, viz. liquid Mercury. The plasma also occurs within the fluorescent lamps and in the lightning, as well as in many laboratory experiments, and in industrial processes. The glow discharge has recently become a backbone of micro-circuit fabrication industry.

1.1 Criteria for Plasmas

The motion of charged particles produce an electric currents which in turn leads to magnetic field, and by which, plasma particles are influenced by the fields of each other, which oversee their collective behaviour with several degrees of freedom [1, 2]. The criteria for a plasma state can be governed by the following characteristics [3, 4]:

1) Plasma frequency

2) Plasma approximation

3) Bulk interactions

1) The oscillation frequency of the plasma particles (the electrons oscillate around the ions with a frequency called the electron plasma frequency) is larger than the frequency due to collisions of the electrons and the neutral particles, viz. $\omega_{pe} > \upsilon_{en}$. This criterion is satisfied when the electrostatic interactions take over the processes of common gas kinetics.

2) The electrons and positively charged ions are strongly affected by the fields of one another, as they are very closed to each other and that also influence many other charged particles in their vicinity. Since the charged particles are not free and therefore are bound, that is why the crowed of the charged particles behaves collectively. Charged particles show a collective motion of large vim and complexity. The plasma approximation becomes important when the number of charged particles in the effective Debye sphere is much greater than unity representing the plasma collective behavior. The effective sphere may be known as the Debye sphere with a radius as the Debye shielding length. The average number of charge particles within the Debye sphere is represented by a Greek letter called Lambda, " Λ ". This condition also tells us that colonial effects are not too large and the plasma dynamics are dominated by the collective forces. However, in a strongly coupled plasma, this condition is relaxed.

3) Initially, the word " Quasi-neutrality " was used in the context of Chemistry in 1907. However, Tonks and Langmuir [5] used this word in Plasma Physics in 1929. For the bulk interactions, it is essential that the Debye screening length of the Debye sphere must be shorter than the dimension (size) of plasma. It means that the interactions due to bulk of plasma are significant as compared to the interactions at the boundaries, where the boundary effects are included. When this condition is satisfied, the plasma will be quasi-neutral. Generally, a plasma is produced due to ionization of neutral gases, and approximately, consists of equal number densities of electrons and positive ions. The positive and negative charge fluids are firmly coupled and must counter balance one another. For a large scale length, they tend to electrically neutralize each other and total electric field within the plasma is zero. As a consequence, the quasi-neutrality arises. Such type of plasma is known as the quasi-neutral plasma. An unmagnitized collisionless plasma having no significant current is known as the simplest plasma. The non-neutral regions are strongly confined and usually situated close to the boundaries. Quasi-neutrality becomes significant at a distance depending on the temperature and the number density of a plasma. The zone of quasi-neutrality becomes smaller if the charged density of a plasma is larger, because it has an equal number of positive and negative charge carriers. The quasi-neutrality breaks down over the Debye length (which is denoted by λ_D). Naturally, the Debye length is less than one millimeter. For different cases, the maximum charge separation or minimum charged neutrality distance can be of the order, for example [6], 10 m for interstellar medium, 10^{-4} m for Tokamak, 10^{-3} m for Ionosphere, 10^{5} m for Intergalactic medium, 10 m for Solar wind, 10^{-4} m for gas discharge tube, 10^{-11} m for Solar core, 10^{2} m for Magnetosphere, etc.

In a rotating plasma, the breaking of quasi-neutrality has been detected when a vortex is formed, called plasma hole [7]. It is noted that the quasi-neutrality breaks down at the center of the plasma hole [8]. Recently, a vortex structure [9] has been studied in a rotating nonplanar magnetoplasma. The spontaneous breaking of charge-neutrality condition takes place in the bulk plasma.

For an ideal plasma, we assume a plasma with equal number of electrons and positive ions. The electronic mass is denoted by m_e and charge by "-e", while M stands for ion's mass with a positive charge "+e". We do not essentially mandate for the system to get thermal equilibrium,

but however we have,

$$T = \frac{1}{3} m_j < v_j^2 >, \tag{1.1}$$

this equation gives a kinetic temperature in the energy units. The kinetic temperature of the particles is necessarily the average kinetic energy of the charged particles and $< v_j >$ represents an average particle speed. The charge-neutrality condition demands that

$$n_i \simeq n_e = n. \tag{1.2}$$

We suppose that the ions and electrons are at equal temperature, ($viz.$ $T_e \sim T_i \sim T$), then the particle thermal speed can be expressed as

$$v_{tj} \equiv (2T/m_j)^{1/2} \tag{1.3}$$

The electron thermal speed is usually much larger than the ion thermal speed due to their large mass difference (i.e. $m_i = 1836 m_e$). That is why, we have

$$v_{ti} \equiv (m_e/m_i)^{1/2} v_{te}, \tag{1.4}$$

where $v_{te} = (2T/m_e)^{1/2}$. On the other hand, The electron plasma frequency can be defined, as

$$\omega_{pe} = \left(\frac{4\pi n e^2}{m_e} \right)^{1/2}. \tag{1.5}$$

This is the most basic time-scale in plasma physics, which arises essentially due to charge separation of plasma particles. Similarly, the electron Debye length (viz. The length time scale) may be expressed, as

$$\lambda_{De} = \left(\frac{T}{4\pi n e^2} \right)^{1/2} \tag{1.6}$$

Thus, an ionized gas (plasma) must satisfy the following necessary conditions:

$$\lambda_{De} << L, \tag{1.7}$$

and

$$\tau_p << \tau \tag{1.8}$$

Here, L and τ show the typical length and time-scales of the system under observation.

1.2 Maxwell's Equations

We consider a set of Maxwell equations in a vacuum as,

$$\nabla \cdot \mathbf{E} = \rho/\epsilon_0, \tag{1.9}$$

$$\nabla \times \mathbf{E} = -\partial_t \mathbf{B}, \tag{1.10}$$

$$\nabla \cdot \mathbf{B} = 0, \tag{1.11}$$

$$\nabla \times \mathbf{B} = \mu_0 \left(\mathbf{J} + \epsilon_0 \partial_t \mathbf{E}\right), \tag{1.12}$$

where μ_0 and ϵ_0 are the permeability and permittivity in a free space, respectively. ρ is the charge density and $\mathbf{J}$ is the current density. The above equations in the presence of a medium having permeability μ_m and permittivity ϵ can be expressed as,

$$\nabla \cdot \mathbf{E} = \rho/\epsilon,\ \nabla \times \mathbf{E} = -\partial_t \mathbf{B},\ \nabla \cdot \mathbf{B} = 0,\ \nabla \times \mathbf{B} = \mu_m \left(\mathbf{J} + \epsilon \partial_t \mathbf{E}\right), \tag{1.13}$$

where $\mathbf{E}$ ($\mathbf{B}$) is the electric field (magnetic field). Plasma is quite different from other the media. Plasma particles behave in a complex manner and their effects in the medium are not countable. Therefore, usually the vacuum equations are used to study the plasma physics.

1.3 Plasma as Dielectric Medium

In order to assume the plasma as dielectric medium, we first define the displacement vector by the relation:

$$\mathbf{D} = \epsilon_0 \mathbf{E} + \mathbf{P}, \tag{1.14}$$

where $\mathbf{P}$ is the polarization vector and can be expressed in terms of electric field vector $\mathbf{E}$ as

$$\mathbf{P} = \epsilon_0 \chi_e \mathbf{E}, \tag{1.15}$$

where χ_e is the electric susceptibility. Using (1.15) into (1.14), we obtain

$$\mathbf{D} = \epsilon_0 \left(1 + \chi_e\right) \mathbf{E} = \epsilon \mathbf{E}, \tag{1.16}$$

where $\epsilon = \epsilon_0 \left(1 + \chi_e\right)$ is a dielectric constant or plasma response function. All the macroscopic properties of the plasma (as a medium) are hidden in the dielectric constant or plasma response function.

1.4 Thermal Plasma

These plasmas have the electron number density in the range $n_e \simeq \left(10^{14} - 10^{19}\right) cm^{-3}$ and the electron temperature $T_e \simeq (0.1 - 2)\, eV$. Both the electrons and ions are nearly in thermal equilibrium having the same temperatures, i.e. $T_e \simeq T_i$. This approximation is valid in laboratory plasmas and under the certain conditions, the local thermal equilibrium can be achieved.

1.5 Cold Plasma

The cold plasmas have the electron temperature $T_e \simeq (1 - 10)\, eV$ and the electron number density in the range $n_e \simeq \left(10^{8} - 10^{13}\right) cm^{-3}$. The electrons are hotter than ions and are not in thermal equilibrium $T_e >> T_i$ because ions have high density and high heat capacity relative to the electrons, therefore, the total heat transmitted to the walls of container and to the background gas is very small. The cold plasma means small amount of heat transmitted to container or gas.

1.6 Dusty Plasma

Dusty plasma is composed of nano-meter or micro-meter particles hanged in it. These dust particles may be electrically charged either negatively or positively depending upon the charging

processes. Thus, a dusty plasma is a plasma containing dust particles, in addition to ions and free electrons. The charge and mass of dust particles may vary as $q_d \sim (10^3 - 10^6)\, e$, and $m_d \sim (10^{-2} - 10^{-15})\, g$, respectively. Dusty plasma is sometimes known as the complex plasma due to complexities regarding the size, mass, charge, and shape.

1.7 Fusion Plasma

In 1952, after the formation of Hydrogen bomb, there was a great motivation of ordered thermonuclear fusion, as a powerful source of energy. The main work to study the fusion plasma, the physicists are trying to know how it can be confined to produce the energy and to use it for peaceful purposes. However, there are two best methods to confine a plasma, one is the inertial confinement fusion (ICF) and the other is the magnetic confinement fusion (MCF).

1.7.1 Laser Produced Plasma

After the invention of high powered laser and its interaction with a solid materials, a new field of physics is opened up known as laser produced plasma physics. The latter has received a great deal of interest of the researchers in recent years. Strong electric fields are produced, when a high powered laser beam interacts with plasma. The plasma particles are accelerated with high energies. High-energy physicists have the large expectations that this plasma technique to accelerate the charged particles can be used to reduce the cost and size of the particle accelerators. In case of fusion, when laser beam hits the solid target, the solid material is ablated and plasma is produced at the surface between the target and laser beam. The laser produced plasma mainly depends on the density of solid target, which is not as very important in most of conventional plasmas as in laser produced plasma. The main focus of laser produced plasma is the ICF, in which the laser beam is focused to explode a tiny solid target up to the temperatures and densities representative of nuclear fusion. The laser beam can enter up to the critical density of plasma, when laser frequency becomes equal to the plasma frequency. For the Nd laser light [10] with $\lambda = 1.06\ \mu m$, the critical surface density exists at $10^{21}\ cm^{-3}$, and the critical surface density occurs at $10^{19}\ cm^{-3}$ for CO_2laser with a wavelength $\lambda = 10.6\ \mu m$.

1.8 Applications and Motivations

Initially, the word plasma was used for an ionized gas by Langmuir [1881-1957]. In the ionized gases, the electrons, ions, and neutral particles reminded him like a blood plasma carried red and white (*cells*) and germs [11]. Langmuir and Tonks were looking into the science of Tungsten-filament light-bulbs, while establishing the theory of plasma sheath. Langmuir found that there are definite periodic variations of electron number density in a plasma discharge tube, which was later known as Langmuir waves. Now-a-days, the Langmuir's work provides the basis in most of the plasma processing, which forms the theoretical basis for manufacturing the combined circuits. After, the Langmuir work, plasma study over the time expanded to many other directions and some of which are narrated in the following:

1.8.1 Natural Plasmas

Theory of evolution of Universe assumes that initially, there was a fireball of fully ionized Hydrogen plasma and Universe came into being after a brutal blast about 10 billion years ago. However, some matter was not in the state of plasma. Most of the stars consist of plasma, like interiors and atmosphere of hot stars, interstellar, planetary nebula, interplanetary media, the outer atmospheres of planets, etc. The natural plasma does not exist on the earth and only occurs in cosmic objects, because in those cosmic objects, plasma has very low number density and very high temperature as compared to the number density and temperature, respectively, on the earth. Moreover, plasma can also be produced in the laboratories. In stars, plasma is bounded by the gravitational force and in the interiors by thermonuclear fusion reactions causing to emit a huge amount of energy, and this energy is transferred in the form of radiations to the outer surface. The magnetic fields exist in all the universe of plasma. The average surface magnetic field of the Sun is nearly of the order 1 to 2 G, but it becomes large in entry and departure points (magnetic fluctuations). Some of the regions, where the plasma naturally exists have been explained below:

Earth's Ionosphere

Earth's ionosphere has the vital role in the context of radio signal broadcasting. It reflects or absorbs the harmful radiations coming out from the sun and acts as a shield against the harmful radiations to protect our life on the earth. Our sun is constantly releasing the radiations which are very intense and consist of Ultra-radiations, $X-rays$ and $\gamma-rays$. When solar wind reaches to the earth's upper atmosphere, it ionizes the upper atmosphere and making a partially ionized gas layer of the Earth known as ionosphere [12]. When the transmitter is over the horizon and emits the radio signal, the latter is reflected back by the plasma in the ionosphere only if the frequency of the radio signal is less than plasma frequency in the ionosphere, therefore the ionosphere is important for communication purposes.

Van Allen Radiation Belts

A belt situated in space in the inner zone of the Earth's magnetosphere and is trapped between the earth's magnetic force lines. James Van Allen had discovered this belt and is now named as Van Allen Radiation Belt. It is a tours containing energetic particles of the plasma around the Earth that come from cosmic rays and solar winds [13]. It is observed that sun and many other stars have also such types of belts. Van Allen Radiation Belt can be divided into two distinct regions. The inner belt contains the combination of energetic protons and high concentration of electrons with energy more than 100 MeV with hundreds of keV, respectively. These are more strongly bounded by the magnetic field than in outer belt [14]. The outer belt contains the energetic electrons and is generally formed by the inward radial diffusion [15, 16], acceleration at local [17], because of allocation of energy from the whistler to the electrons of the outer belt. The electrons of the outer belt may be continuously removed by the collisions of neutral particles of atmosphere [18] and due to the outward radial diffusion.

Aurora

Aurora is a natural light known as the northern and southern lights appearing in the sky about 50 miles above the surface of the Earth. The charged particles are accelerated into the upper atmosphere of earth parallel to the magnetic field lines of the earth, colliding with a large energy. Atoms are excited and light photons are emitted during the de-excitation. Generally,

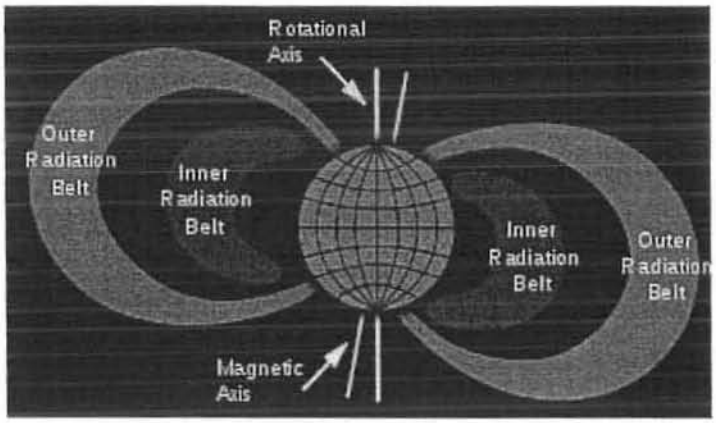

Figure 1-1: Van Allen radiation belt

aurora appears in a band known as auroral zone [19, 20].

Corona

It is the plasma in the atmosphere of the sun; corona is present outside the chromospheres and spreads into the solar wind. There is a temperature of million Kelvins around the sun in the corona region. In spite of energy reduction due to conduction and radiation, the temperature of this region remains at the million Kelvin. Actually, it is a challenging assignment for the researchers to discover the solar corona heating source. The active regions are the loop arrangement joining the points in the photosphere of opposite magnetic polarity, are known coronal loops. The density varies from 10^9 to 10^{10} particles/ cm^3, with an average temperature in the range (2-4) million Kelvin. The active regions contain all the incidents directly associated to the magnetic field, existing at various heights on the surface of the Sun [21], Corona is the main arrangement of the coronal loops. These coronal loops actually contain closed magnetic flux counterpart of the open magnetic flux observed in solar wind and coronal polar zone, spreading up in the form of loops from solar body [22].

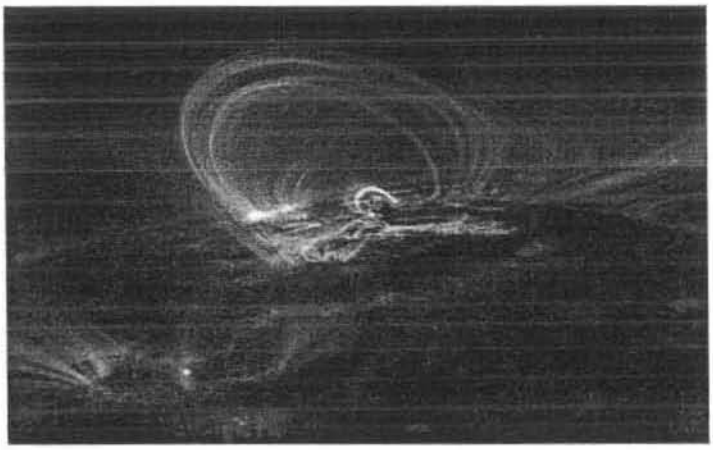

Figure 1-2: Coronal loops

H II Regions

In the neighborhood of a hot star, some medium known as the interstellar medium completely comprised of fully ionized Hydrogen gas. The temperature of this region is so high, and the Hydrogen gas is ionized by the ultraviolet radiations of the neighboring star. Such zones are known as H II regions. Far away from interstellar medium, there are big neutral Hydrogen clouds, and are known as H I regions, while the cosmic rays and dust particles are the remaining parts of the interstellar medium.

1.9 Fluid Equation in Plasmas

In the fluid model, the fluid behavior of the particles is studied instead of individual particle behavior. Let us suppose that a plasma fluid with n_j, the number density of the jth species (j equals e for electrons, and i for ions) and fluid velocity $\mathbf{v}_j$. Then, the continuity equation can be written as,

$$\partial_t n_j + \nabla \cdot (n_j \mathbf{v}_j) = 0, \tag{1.17}$$

The momentum equation is

$$\partial_t \mathbf{v}_j + (\mathbf{v}_j \cdot \nabla)\mathbf{v}_j = \frac{q_j}{m_j}\left(\mathbf{E} + \frac{\mathbf{v}_j \times \mathbf{B}}{c}\right) - \frac{\nabla p_j}{n_j m_j}, \tag{1.18}$$

and the Poisson equation, as

$$\nabla \cdot \mathbf{E} = 4\pi \sum_j q_j n_j, \tag{1.19}$$

where the pressure force term (∇p_j) is due to thermal motion of the plasma species and the pressure $p_j = n_j k_B T_j$. T_j is the temperature and k_B is the Boltzmann constant. $\mathbf{E} = -\nabla V(\mathbf{r}, t)$ is the induced electric field with an electrostatic potential V. However, by neglecting the magnetic field effects and using the linear theory, i.e. $n_j = n_{j0} + n_{j1}$, $\mathbf{v}_j = \mathbf{v}_{j1}$, $\mathbf{E} = \mathbf{E}_1$, and $V = V_1$, the linearized fluid equations becomes

$$\partial_t n_{j1} + n_{j0} \nabla \cdot \mathbf{v}_{j1} = 0, \tag{1.20}$$

$$\partial_t \mathbf{v}_{j1} = \frac{q_j}{m_j} \mathbf{E}_1 - \frac{k_B T_j}{m_j n_{j0}} \nabla n_{j1}, \tag{1.21}$$

and

$$\nabla \cdot \mathrm{E}_1 = 4\pi \sum_j q_j n_{j1}, \tag{1.22}$$

On the ion time-scale, the electrons can be assumed as massless, or inertialess in comparison with ions and can be described by the linearized Boltzmann equation as,

$$n_{e1} \simeq n_{e0} \exp\left(\frac{eV_1}{k_B T_e}\right) \tag{1.23}$$

1.10 Group and Phase Velocities

To study the waves in plasmas, one must know about the velocities of the waves, i.e. the group velocity and the phase velocity. Phase velocity is the velocity at which the planes of wave move with constant phase. It is very astonishing and unbelievable thing to know that in plasma the phase velocity of a wave frequently surpasses the velocity of light. However, modulated waves propagate with group velocity instead of phase velocity. Group velocity is always smaller than the light speed c. In quantum mechanics, the velocity of a confined particle is called its group velocity [26]. Because it changes with wave vector k, the particle becomes less confined, and the wave packet's shape expands [27] as shown in the Fig. 1.3.

The phase and group velocities [27, 28, 29, 30] can be given in terms of wave frequency and

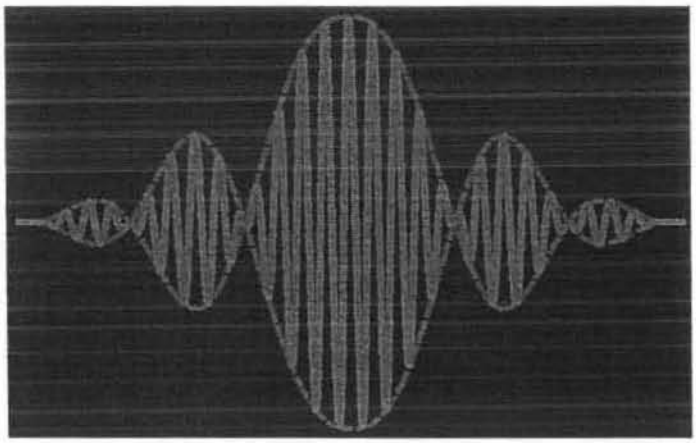

Figure 1-3: Group velocity

wave number, respectively, as

$$v_p = \omega/k,\ v_g = d\omega/dk. \tag{1.24}$$

It is noted that if the angular frequency of wave is directly proportional to wavenumber, then the group velocity of wave is absolutely equal to its phase velocity. The refractive index may be defined in terms of phase velocity by the relation $n = c/v_p = ck/\omega$.

1.11 Alfven Theory

The Astrophysicists know that most of the Universe comprises of plasma that is why, they feel that there should be a better grip on plasma physics to solve the astrophysical phenomena. Hannes Alfvén established a magnetohydrodynamics (MHD) theory [23] in 1940 for which, he got the Nobel Prize in 1970 in physics. In his theory, the plasma is basically assumed as a conducting fluid and when it is kept in a constant magnetic field, the electromagnetic forces are produced by the every movement of fluid, giving rise to electrical currents, which provide the mechanical forces through which the fluid's state of motion changes. Thus, a joint hydrodynamic-electromagnetic wave is generated [24]. This is a very successful theory and is used to study the star formation, solar wind, solar flares, and sunspots. The MHD theory can be important in the context of dynamo theory and in the magnetic reconnection. The Alfven

waves are extremely low frequency waves [25] which occur in the presence of a magnetic field.

1.12 Electron Plasma Wave

The electron wave is mainly produced due to dynamics of electrons in plasma in the presence of static ions. In order to study the electron plasma wave, the phase speed must be larger than electron thermal speed, viz. $\omega \gg kS_e$. The dispersion relation for the electron wave can be expressed, as

$$\omega^2 = \omega_p^2 + \frac{3}{2}k^2 S_e^2, \tag{1.25}$$

where $S_e = (2k_B T_e/m_e)^{1/2}$ is the electron thermal speed and $\omega_{pe} \equiv \left(4\pi n_{e0} e^2/m_e\right)^{1/2}$ is the electron plasma frequency.

1.13 Electron-Acoustic Wave

This type of wave is produced in a two-temperature plasma. The ions are treated as stationary particles whereas the cold electrons are mobile and the hot electrons are assumed to obey the Boltzmann distribution. The phase velocity of the wave lies between the thermal speed of cold and hot electrons, (viz. $S_c << \omega/k << S_h$). Where $S_c = (2K_B T_c/m_c)^{1/2}$ and $S_h = (2K_B T_h/m_h)^{1/2}$ are the cold and hot electron thermal speeds. T_c (T_h) is the cold (hot) electron temperature. The electron-acoustic (EA) wave has a dispersion relation, as

$$\omega = \frac{kC_e}{\left(1 + k^2\lambda_{Dh}^2\right)^{1/2}}, \tag{1.26}$$

where $C_e = (\omega_{pc}\lambda_{Dh})$ is the EA speed, λ_{Dh} is the hot electron Debye length, and ω_{pc} is the cold electron plasma frequency.

1.14 Ion-Acoustic Wave

We are interested in the dynamics of ions, the later as compared to electrons. At such a time-scale the electrons are assumed to follow the Boltzmann distribution. The phase speed of IA wave lies in between the electron and ions thermal speeds as, $S_i \ll \omega/k \ll S_e$. The dispersion

relation for IA wave is given by

$$\omega = \frac{kC_s}{\left(1 + k^2\lambda_{De}^2\right)^{1/2}}, \tag{1.27}$$

where $C_s = \omega_{pi}\lambda_{De}$ is the IA speed and λ_{De} is the electron Debye length.

1.15 Light Wave

Light wave comprises of a stream of photons and is an electromagnetic wave. The dispersion relation for light wave in a plasma medium is given by

$$\omega^2 = \omega_{pe}^2 + k^2c^2, \tag{1.28}$$

where ω (k) is the angular frequency (wave number) of light wave.

1.16 Planar and Helical Wavefronts

The wavefronts of the laser beams can be assumed as planar and helical depending on the following properties:

1.16.1 Planar Wavefronts

- In laser light, the wavefronts are usually planar with uniform phase.
- The wavevectors and linear momentum of the photons are directed along the beam axis.
- Each photon has angular momentum of $\sigma_z\hbar$ aligned parallel or antiparallel to the direction of propagation.
- Alignment of all the photon spins gives rise to circularly polarized light beam.

1.16.2 Helical Wavefronts

- Laser beams with helical wavefronts have wavevectors which spiral around the beam axis and give rise to OAM.

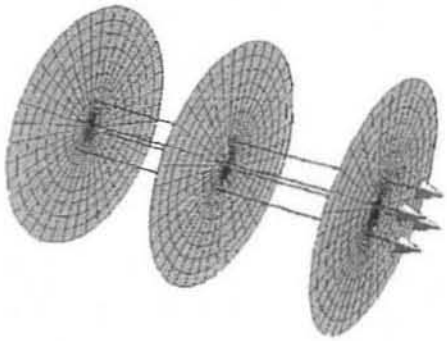

Figure 1-4: Light with planar wavefronts.

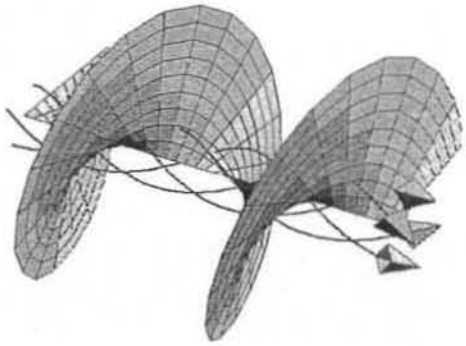

Figure 1-5: Light with helical wavefronts

- Helical wavefronts are also circularly polarized and showing the total angular momentum $(l + \sigma_z)\hbar$ per photon [31].
- l is the number of intertwind helices and σ_z is the spin polarization.
- Helical wavefronts [32] can be represented in a basis set of orthogonal Laguerre-Gaussian (LG) beams.
- Each LG beam is associated with a well-defined state of photon OAM.

With the invention of laser beam, the photon OAM and many other optical phenomena have been studied [32, 33, 34, 35].

1.17 Laguerre-Gaussian Beams

Any laser beam can be described by a Laguerre Gaussian beam [37], which represents a general solution of the paraxial wave equation in cylindrical geometry. By using the Laguerre polynomials, the Laguerre Gaussian beam can be described in the form of cylindrical coordinates (r, ϕ, z) as

$$\begin{aligned} u(r,\phi,z) &= \frac{C_{lp}^{LG}}{\omega(z)}\left(\frac{r\sqrt{2}}{\omega(z)}\right)^{|l|}\exp\left(-\frac{r^2}{\omega^2(z)}\right)L_p^{|l|}\left(\frac{2r^2}{\omega^2(z)}\right) \\ &\quad \times \exp\left(ik\frac{r^2}{2R(z)}\right)\exp(il\varphi)\exp\left[-i\left(2p+|l|+1\right)\zeta(z)\right], \end{aligned} \tag{1.29}$$

where $\zeta(z)$, $R(z)$ and $\omega(z)$ are the beam parameters. $L_p^{|l|}$ are the generalized Laguerre polynomials, C_{lp}^{LG} is an appropriate normalization constant, l is the azimuthal quantum number and $p \geq 0$ is the radial quantum number. The characteristics of LG beams can be studied in the following way:

- LG beams are the natural orthonormal basis set represented in cylindrical geometry.
- If the beam is not a perfect Gaussian, then higher order terms are included in the intensity profiles of LG modes giving rise to OAM.
- The LG beams are circular symmetric about the beam axis.
- The phase structure is described by the azimuthal index "l ".
- For $l \neq 0$, the LG beams have helical wavefronts with a handedness which is linked to the sign of "l ", can be chosen by convention.
- The phase variation around the beam centre is $2\pi l$.
- The phase singularity on the beam axis leads to zero axial intensity for $l \neq 0$.
- The radial structure is described by the radial index " p ".
- For $p = 0$, the LG beam gives a ring like profile and for higher values of p, the multi-ringed profiles with $(p + 1)$ rings are obtained.

- For assuming $l = 0 = p$, the lowest order beam LG_0^0 known as Gaussian beam can be recovered.

1.18 Angular Momentum

Experimental studies [38] have confirmed the presence of the orbital angular momentum (OAM) by inserting the spiral phase plate to change the Guassian modes into the Laguerre Guassian modes containing the azimuthal phase term $\exp(il\varphi)$. In 1936, Beth, experimentally studied [39] the mechanical torque created due to the interchange of angular momentum to a half-wave plate. The photon angular momentum [45] is essentially composed of two parts, one the spin angular momentum due to polarization states and the other is the orbital angular momentum which is produced due to angular phase structure of the wavefronts. Hence, the total angular momentum involving the photon beam is the sum of the spin and orbital angular momenta i.e. $M = (l + \sigma_z)\hbar$, where $\sigma_z(= \pm 1)$ indicates the left and right handed circularly polarized light. The spin angular momentum becomes zero ($\sigma_z = 0$) for linearly polarized light. Moreover, $l(= 0, \pm 1)$ is the quantum number of the orbital angular momentum, which corresponds to the azimuthal index of the LG modes. It has been noticed that the electrostatic waves (like plasmons [52], phonons [56], etc.) do not possess any spin angular momentum besides the orbital angular momentum due to their longitudinal nature of propagation. Since the electromagnetic waves (photons) are the transverse waves and therefore carry both spin and orbital angular momenta. Very recently, Shukla [76] has explained the twisted shear Alfven waves with orbital angular momentum states.

1.19 Layout of Thesis

In the first Chapter, we have studied about the plasma and briefly described its properties and criteria. Different types of the plasmas have been explained and presented the dispersion relations of well-known plasma waves, such as, the light waves, the electron waves, the ion-acoustic waves, etc. Furthermore, the spin and orbital angular momenta, the Laguerre-Gaussian beams, and the properties of the planar and helical wavefronts are discussed in details.

Second Chapter explains the of ion-acoustic waves (IA) or phonons with orbital angular

momentum in an unmagnetized collisionless uniform plasma. For this purpose, fluid equations for ions are employed derive a linear dispersion relation for phonons in the paraxial approximation. A beam as well as Laguerre Gaussian solutions are used to analyze the properties of LG phonons. The electrostatic potential problem is solved in the context of paraxial approximation to obtaining the electric field components in terms of LG potential. Furthermore, the energy density, energy flux, and the angular momentum density of the phonon modes are computed analytically and presented numerically.

Third Chapter the studies of the Raman and Brillouin backscattering of the beams carrying the orbital angular momentum. For this, the nonlinear dispersion relations of electromagnetic and electron plasma waves are derived and coupled together. Using the paraxial approximations, the coupled equations are solved for Laguerre Gaussian modes and the growth rates for the backscattered transverse and electrostatic waves are derived. We have also considered the coupling of the electromagnetic waves with the ion-acoustic waves (phonons) and obtained the growth rates.

The last Chapter discusses the extension of phonon beam's study to electron-acoustic (EA) wave carrying a finite amount of orbital angular momentum in a two-temperature electron unmagnetized plasma. The usual dispersion relation of the EA wave is employed to obtain an approximate paraxial equation for EA waves. The electrostatic potential problem is solved for Laguerre-Gaussian beam solutions. The expressions for the energy flux and the angular momentum involving EA waves are presented in an unmagnetized collisionless plasma. Numerically, the Laguerre-Gaussian potential profiles are examined for the variation of azimuthal and radial mode numbers.

Chapter 2

Ion-Acoustic Waves with Orbital Angular Momentum

2.1 Introduction

There is a growing interest relating to studying the light-matter interaction [40]. The interactions or the exchange of angular momentum between the electrostatic and electromagnetic waves has been studied extensively [41, 42, 43, 44] in a plasma. In 1936, Beth and Holbourn experimentally computed [39] the mechanical torque by the exchange of angular momentum to a half wave plate. Allen et al. [45] theoretically investigated the orbital angular momentum (OAM) involving the photon beams by employing Laguerre-Gaussian beams. Just like energy and momentum, the angular momentum can also be never created nor destroyed but only be exchanged. First time, Mendonca et. al [46] presented the angular momentum states for phonon and plasmon fields, which may be excited by the nonlinear wave mixing, involving the scattering phenomena. They derived nonlinearly coupled paraxial wave equations and instability growth rates in the paraxial approximations. Brillouin and Raman instabilities are very famous in the application of laser fusion [47]. Courtial et al. [48] explained the rotational frequency shift, when the angular momenta (spin and orbital angular momentum) are added to the plasma beam. It is found that the angular momentum associated with the electromagnetic radiations comprises of two distinct parts, one is related to polarization (due to transverse part of electromagnetic radiation) or spin and the other is the photon orbital part due to angular

phase structure [32, 33, 34, 35, 49]. Similarly, photon beams carrying spin and orbital angular momenta related to electromagnetic fields have been studied in both classical and quantum electrodynamics [50, 51]. In this Chapter, we will be interested to study ion-acoustic waves carrying a finite amount of OAM in an unmagnetized collisionless uniform plasma. For this purpose, we will consider the dynamics of mobile ions and assuming the electrons as Boltzmann distributed. The cherge-neutrality at equilibrium imposes the condition $n_{e0} = n_{i0}$. Since we are interested in the IA waves on a time scale longer than the electron plasma period, therefore, the wave phase speed can be described as $S_i \ll \omega/k \ll S_e$, where S_i (S_e) is the ion (electron) thermal speed.

2.2 Dispersion Relation for Phonons (Ion-Acoustic Waves)

To calculate the dispersion relation of the ion-acoustic waves or phonons, we consider an unmagnetized collisionless plasma containing the electrons and ions. The ions are described by the fluid equations (The continuity and momentum equations), whereas the electrons are assumed to follow the Boltzmann distribution. The linear dynamics of the ion-acoustic waves is governed by the following fluid equations:

$$\partial_t n_{i1} + n_{i0}\nabla \mathbf{v}_{i1} = 0, \tag{2.1}$$

$$\partial_t \mathbf{v}_{i1} = \frac{e}{m_i}\mathbf{E} - \frac{S_i^2}{n_{i0}}\nabla n_{i1}, \tag{2.2}$$

and

$$\nabla\cdot\mathbf{E} = 4\pi e(n_{i1} - n_{e1}). \tag{2.3}$$

Here n_{i1} shows ion number density perturbations with an equilibrium part n_{i0}. $\mathbf{E} = -\nabla V(\mathbf{r}, t)$ is the electric field, $V(\mathbf{r}, t)$ is the induced electrostatic potential, $S_i = (k_B T_i/m_i)^{1/2}$ the ion thermal speed, and $\mathbf{v}_{i1}$ stands for the ion fluid velocity. The perturbed electron density may be approximated by the Boltzmann distribution in the limit $eV/k_B T_e << 1$, as

$$n_{e1} \simeq n_{e0}\frac{eV}{k_B T_e}. \tag{2.4}$$

Here $n_{e1}(\ll n_{e0})$ is the perturbed electron number density with equilibrium state n_{e0}, T_e and T_i are the electron and ion temperatures, respectively, k_B denotes the Boltzmann constant.

Taking the time derivative of Eq. (2.1), we obtain

$$\frac{\partial}{\partial t}\nabla \cdot \mathbf{v}_{i1} = -\frac{1}{n_{i0}}\frac{\partial^2 n_{i1}}{\partial t^2} \tag{2.5}$$

Equation (2.2) after taking divergence can be combined to (2.5), obtaining

$$\left(\frac{\partial^2}{\partial t^2} - S_i^2\nabla^2\right) n_{i1} = \frac{en_{i0}}{m_i}\nabla^2 V \tag{2.6}$$

Substituting (2.4) into (2.3), we get

$$\left(\frac{1-\nabla^2\lambda_{De}^2}{\lambda_{De}^2}\right) V = 4\pi n_{i1}, \tag{2.7}$$

where $\lambda_{De} = (k_B T_e/4\pi e n_{e0})^{1/2}$. For long wave length limit, i.e. $\nabla^2\lambda_{De}^2 \ll 1$, the electrostatic potential gives

$$V = 4\pi n_{i1}\lambda_{De}^2 \tag{2.8}$$

Assuming that $\partial^2 n_{i1}/\partial t^2 \gg S_i^2\nabla^2 n_{i1}$ and combining Eq. (2.8) with (2.6), we have

$$\left(\frac{\partial^2}{\partial t^2} - C_s^2\nabla^2\right) n_{i1}(\mathbf{r}, t) = 0. \tag{2.9}$$

Equation (2.9) describes the ion number density perturbations with an ion-acoustic speed $C_s = \omega_{pi}\lambda_{De} \equiv (k_B T_e/m_i)^{1/2}$.

2.3 Paraxial Equation for Ion-Acoustic Waves/ Phonons

In order to study orbital angular momentum and the paraxial equation for the ion-acoustic waves, we consider a beam type solution as given in the following form:

$$\tilde{n}_{i1}(\mathbf{r}, t) = \tilde{n}_0(\mathbf{r})\exp\left(ik_z z - i\omega t\right), \tag{2.10}$$

where $\tilde{n}_0(\mathbf{r})$ is a slowly varying amplitude in spatial coordinate describing the wave profile. Decomposing the operator ∇ in Eq. (2.9) into its perpendicular and parallel components, that is, $\nabla = \nabla_\perp + \hat{z}\partial/\partial z$, one obtains a Helmholtz equation without any approximation

$$\left(\nabla^2 + k_z^2\right) \tilde{n}_{i1}(\mathbf{r}, t) = 0, \tag{2.11}$$

where $k_z^2 (= \omega^2/C_s^2)$ is the longitudinal wave number squared and ω is the angular wave frequency of the IA mode. Equation (2.11) can be described as parsed Helmholtz equation

$$\nabla_\perp^2 \tilde{n}_0(\mathbf{r}) + \frac{\partial^2}{\partial z^2}\tilde{n}_0(\mathbf{r}) + 2ik_z \frac{\partial}{\partial z}\tilde{n}_0(\mathbf{r}) = 0. \tag{2.12}$$

For the paraxial approximation i.e. $\partial^2 \tilde{n}_0(\mathbf{r})/\partial z^2 \ll 2ik_z \partial \tilde{n}_0(\mathbf{r})/\partial z$, Eq. (2.12) reduces to

$$\left(\nabla_\perp^2 + 2ik_z \frac{\partial}{\partial z}\right) \tilde{n}_0(\mathbf{r}) = 0. \tag{2.13}$$

Here, the paraxial approximation means that the wavelength ($\lambda = 2\pi/k_z$) associated to $\tilde{n}_0(\mathbf{r})$ changes very little along the longitudinal direction (z-axis). Equation (2.13) also satisfies the linear dispersion relation of the ion-acoustic waves $\omega^2 = C_s^2 k_z^2$. The transverse Laplacian operator can be expressed into cylindrical coordinates, as $\nabla_\perp^2 = (1/r)(\partial/\partial r)(r\partial/\partial r) + (1/r^2)\partial^2/\partial\varphi^2$, to obtain an axially symmetric beam solution in the form of Gaussian function, as

$$\tilde{n}_0(\mathbf{r}) = \tilde{n}_0(r, z) \equiv N_0(z) \exp\left(\frac{ik_z r^2}{2R(z)}\right), \tag{2.14}$$

with $N_0(z)$, the maximum amplitude associated with Gaussian beam, $R(z)$, the complex beam waist and $r^2 = x^2 + y^2$ is the radial coordinate squared. Now using this solution into Eq. (2.13), we obtain

$$\left\{2ik_z\left(\frac{1}{R} + \frac{1}{N_0}\frac{dN_0}{dz}\right) + \frac{k_z^2 r^2}{R^2}\left(\frac{dR}{dz} - 1\right)\right\} \tilde{n}_0(\mathbf{r}) = 0, \tag{2.15}$$

Equation (2.15) is thus satisfied, when $N_0(z) = \frac{N_0(0)R_0}{R(z)}$ and $R(z) = R_0 + z - z_0$. Here $N_0(0)$, the maximum wave amplitude at focal position ($z = z_0$) and R_0 the minimum beam waist. Thus the solution may be written in the following form

$$\tilde{n}_0(\mathbf{r}) = \tilde{n}_0(r,z) \equiv \frac{N_0(0)}{1+(z-z_0)/R_0} \exp\left(\frac{1}{2}\frac{ik_z r^2}{R_0+z-z_0}\right). \tag{2.16}$$

This is the lowest order mode of the LG solution carrying zero orbital angular momentum. For incorporating the latter, we have to study the higher order modes of LG solutions involving the well-defined orbital angular momenta. To express (2.13) in terms of LG functions, which represents a more general solution for the paraxial equation. The LG solutions may be described as

$$\tilde{n}_0(r,\varphi,z) = \frac{\tilde{N}_0}{2\sqrt{\pi}} \left\{\frac{(l+p)!}{p!}\right\}^{\frac{1}{2}} X^{|l|} L_p^{|l|}(X) \exp\left(-\frac{X}{2}\right) \exp(il\varphi), \tag{2.17}$$

where $X = r^2/\omega^2(z)$. $\omega(z)$ denotes the IA beam width. $\tilde{N}_0$ stands for maximum amplitude involving IA mode at focal position, $l = 0, \pm 1, \pm 2, ...$ and $p = 0, 1, 2, ...$ show the angular and radial quantum numbers, and φ is the azimuthal angle.

One can expressed the associated Laguerre polynomials into Rodrigues formula, as

$$L_p^{|l|}(X) = \exp(X)\frac{X^{-l}}{p!}\left[\frac{d^p}{dX^p}\left\{X^{l+p}\exp(-X)\right\}\right] \tag{2.18}$$

Assuming a special case, $p = 0$, $l = 0$ and $R(z) = ik_z\omega^2(z)$, the lowest order mode i.e. the Gaussian beam solution can be retrieved [52]. Equation (2.17) in a more simple form can be described as,

$$\tilde{n}_0(\mathbf{r},t) = \tilde{n}_{pl}(z)\exp(il\varphi + ikz - i\omega t), \tag{2.19}$$

where $\tilde{n}_{pl}(z) = \tilde{N}_0 F_{pl}(r,z)$ with $F_{pl}(r,z) \equiv \frac{1}{2\sqrt{\pi}}\left\{\frac{(l+p)!}{p!}\right\}^{\frac{1}{2}} X^{|l|} L_p^{|l|}(X)$, the Laguerre Gaussian or mode structure function. Thus, in the phonon beam, the wavefront would rotate around the beam axis in a spiral, looking like a fusilli pasta and giving rise to zero intensity at the beam centre.

2.4 Electrostatic Potential Problem

To investigate the IA mode or phonon mode with a well-defined angular momentum (viz. $l \neq 0$), we demonstrate the electrostatic potential in term of LG functions. In this context, the

Poisson's equation is considered in which the electrons are assumed to follow the Boltzmann distribution, whereas the ions are treated as dynamic. Thus, we may write the electrostatic potential associated with the electron and ion density perturbations, as

$$\nabla^2 V(\mathbf{r},t) = -4\pi e(n_{i1} - n_{e1}) \tag{2.20}$$

One can express the electrostatic potential $V(\mathbf{r},t)$ in terms of LG functions as

$$V(\mathbf{r},t) = V_{pl}(r,z)e^{(il\varphi + ik_z z - i\omega t)}, \tag{2.21}$$

where the amplitude of the electrostatic potential corresponds to $V_{pl}(r,z) = \tilde{V}_0 F_{pl}(r,z)$. Substituting (2.4) and (2.21) into (2.20), a simplified form is obtained by noting $\nabla^2 = \nabla_\perp^2 - k_z^2 + 2ik_z\frac{\partial}{\partial z}$, as

$$\left\{\left(\nabla_\perp^2 + 2ik_z\frac{\partial}{\partial z}\right) - k_z^2 - \frac{1}{\lambda_{De}^2}\right\} V(\mathbf{r},t) = -4\pi e n_{i1} \tag{2.22}$$

This equation can easily be solved by applying the paraxial equation similar to Eq. (2.13), obtaining

$$\left(\nabla_\perp^2 + 2ik_z\frac{\partial}{\partial z}\right) V(\mathbf{r},t) = 0, \tag{2.23}$$

Thus, Eq. (2.22) may be reduced to

$$V(\mathbf{r},t) = 4\pi e\left(\frac{\lambda_{De}^2}{1 + k_z^2\lambda_{De}^2}\right)\tilde{n}_{i1} \tag{2.24}$$

This represents a relation between LG density perturbations and the amplitude of the LG potential perturbations. LG density perturbations help to determine the amplitude

$$\tilde{V}_0 = \frac{4\pi e\tilde{N}_0\lambda_{De}^2}{1 + k_z^2\lambda_{De}^2}. \tag{2.25}$$

Note that the amplitude of the LG potential is appreciably modified due to the occurrence of the Boltzmann electrons through the Debye shielding length. Now we can express electric field

in terms of Laguerre Gaussian potential by the relation

$$\mathbf{E}(\mathbf{r},t) = -\nabla V(\mathbf{r},t). \tag{2.26}$$

With its components into cylindrical coordinates

$$\begin{aligned} E_r &= -\frac{V}{F_{pl}}\frac{\partial F_{pl}}{\partial r}, \\ E_\varphi &= -i\frac{lV}{r}, \\ E_z &= -\left\{ik_z + \frac{1}{F_{pl}}\frac{\partial F_{pl}}{\partial r}\right\}V \end{aligned} \tag{2.27}$$

Similarly, in the usual way, the electric field may be expressed, as

$$\mathbf{E} \equiv -i\mathbf{k}_{ef}V(\mathbf{r},t). \tag{2.28}$$

Here, $\mathbf{k}_{ef}$ stands for the effective wave number and is given by

$$\mathbf{k}_{ef} = -\frac{i}{F_{pl}}\left(\frac{\partial F_{pl}}{\partial r}\right)\hat{\mathbf{e}}_r + \frac{l}{r}\hat{\mathbf{e}}_\varphi + \left\{k_z - \frac{i}{F_{pl}}\left(\frac{\partial F_{pl}}{\partial r}\right)\right\}\hat{\mathbf{e}}_z. \tag{2.29}$$

The radial, azimuthal, and axial unit vectors are denoted by $\hat{\mathbf{e}}_r$, $\hat{\mathbf{e}}_\varphi$, and $\hat{\mathbf{e}}_z$, respectively. In the following we shell calculate the energy flux and OAM associated with ion-acoustic mode or phonon mode.

2.5 Energy Flux and OAM Of Ion-Acoustic Wave

When an ion-acoustic mode propagates in an unmagnetized collisionless uniform plasma, it carries a finite amount of orbital angular momentum. The spin angular momentum associated with the ion-acoustic wave is zero because of its electrostatic nature. The energy density [52] for Laguerre-Gaussian IA mode can be obtained by considering the dispersive properties of the plasma medium, as

$$W = \frac{\mid E \mid^2}{8\pi} \frac{\partial}{\partial \omega} (\epsilon \omega), \tag{2.30}$$

and energy flux is given [52] by

$$\mathbf{T}_p = W v_g \hat{\mathbf{e}}_{ef}, \tag{2.31}$$

where $\hat{\mathbf{e}}_{ef} (= \mathbf{k}_{ef} / \mid k_{ef} \mid)$ is the effective unit vector along the electric field, v_g denotes the group velocity of the IA wave. The dielectric response function of IA wave is giving by

$$\epsilon(\omega, k_z) = 1 + \frac{1}{\lambda_{De}^2 k_z^2} - \frac{\omega_{pi}^2}{\omega^2 - S_i^2 k_z^2}, \tag{2.32}$$

where $\lambda_{De} = S_e / \omega_{pe}$. Thus, the expression for the energy density becomes, as

$$W = \frac{\mid E \mid^2}{8\pi} \left\{ 1 + \frac{1}{\lambda_{De}^2 k_z^2} + \frac{\omega_{pi}^2 \left(\omega^2 - S_i^2 k_z^2\right)}{\left(\omega^2 - S_i^2 k_z^2\right)^2} \right\}. \tag{2.33}$$

To describe the energy density in terms of LG potential, we use the relation

$$\mid E \mid^2 = \mathbf{E} \cdot \mathbf{E}^* \equiv k_{ef}^2 \mid V \mid^2 . \tag{2.34}$$

One can express the angular momentum density in terms of average of linear momentum density in cylindrical coordinates, as

$$\mathbf{M}(\mathbf{r}) = \mathbf{r} \times < \mathbf{P} >, \tag{2.35}$$

where

$$< \mathbf{P} > = \frac{< \mathbf{T}_p >}{v_g^2} \equiv \frac{< W > \hat{\mathbf{e}}_{ef}}{v_g} \tag{2.36}$$

Combining Eqs. (2.33) and (2.34) and substituting into Eq. (2.36), we get

$$< \mathbf{P} > \equiv \frac{k_{ef}^2 <\mid V \mid^2>}{8\pi v_g} \left\{ 1 + \frac{1}{\lambda_{De}^2 k_z^2} + \frac{\omega_{pi}^2 \left(\omega^2 + S_i^2 k_z^2\right)}{\left(\omega^2 - S_i^2 k_z^2\right)^2} \right\} \hat{\mathbf{e}}_{ef}. \tag{2.37}$$

Using Eq. (2.37) into Eq. (2.35) and after doing some straightforward algebra, we obtain

$$\mathrm{M(r)} = \frac{|\, k_{ef} \,|<|\, V(\mathbf{r}) \,|^2>}{8\pi v_g}\left[-\frac{lr_{\parallel}}{r}\hat{\mathrm{e}}_r - \left\{\frac{ir_{\parallel}}{F_{pl}}\frac{\partial F_{pl}}{\partial r} + rk_z - \frac{ir}{F_{pl}}\frac{\partial F_{pl}}{\partial z}\right\}\hat{\mathrm{e}}_{\varphi} + l\hat{\mathrm{e}}_z\right] \times \left\{1 + \frac{1}{\lambda_{De}^2 k_z^2} + \frac{\omega_{pi}^2\left(\omega^2 + S_i^2 k_z^2\right)}{\left(\omega^2 - S_i^2 k_z^2\right)^2}\right\}. \tag{2.38}$$

The axial part of (2.38) along the direction of propagation of the longitudinal IA beam is practically important, which is proportional to the angular mode number l, similar to the case of photons [53] as

$$M_z = l\frac{|\, k_{ef} \,|<|\, V(\mathbf{r}) \,|^2>}{8\pi v_g}\left[1 + \frac{1}{\lambda_{De}^2 k_z^2} + \frac{\omega_{pi}^2\left(\omega^2 + S_i^2 k_z^2\right)}{\left(\omega^2 - S_i^2 k_z^2\right)^2}\right] \tag{2.39}$$

Note that M_z is directly proportional to the magnitude of Laguerre Gaussian potential and inversely proportional to the phonons group velocity. If we consider that the angular mode number $l = 0$, then angular momentum density vanishes. Hence the lowest order mode is a pure Gaussian mode with no OAM. However, for higher order modes ($l \neq 0$), a finite amount of OAM is associated with the IA beam. Equation. (2.25) exhibits that the amplitude of Laguerre Gaussian potential is generally dependent on the ion density perturbations and the electron Debye shielding length, playing an important role in the IA orbital angular momentum states.

2.6 Numerical Analysis of IA Waves:

In this section, we numerically plot LG potential V(r) associated with the IA waves (phonons) as a function of " r ", and choose some typical values from the laboratory plasma [54] such as $T_e \simeq 3 \times 10^4 K$, and $n_{e0} = n_{i0} \simeq 10^{12} cm^{-3}$. By using these values, we find $\omega_{pi} \simeq 1.4 \times 10^8 s^{-1}$, $\omega_{pe} \simeq 2 \times 10^{10} s^{-1}$ and $\lambda_{De} \sim 10^{-3} cm$. Assuming that ion density perturbation, viz. $\tilde{N}_0/n_{i0} \sim 0.1$, which leads to calculate the amplitude of LG potential as $\tilde{V}_0 \sim 8.3 \times 10^{-4}$V with IA beam waist $\omega_0 = 3\lambda$, where $\lambda = 10\ cm$ is the wavelength of phonons. Figure (2.1) depicts the variation in LG potential V(r) caused by phonon beam, as a function of r at the focal point for $t = 0$. For assuming $l = 0 = p$, the lowest order of the LG potentials (Gaussian profiles) are obtained

for varying IA beam width $\omega_0(= 2\lambda, 3\lambda, 4\lambda, 5\lambda, 6\lambda)$. It is noted that the amplitude of the LG potential remains the same but width of profiles increases with the increase in the IA beam waist. However, for $l = 0$ and $p \neq 0$, the profiles become a non-Gaussian. It is significant to note that the amplitude of the Laguerre Gaussian potential due to the phonon modes remains constant while IA beam width decreases for increasing radial index p. It is examined that the number of nodes on both sides increases with increasing the value of radial index p as shown in the Fig. 2.2. Firgure 2.3 shows the effect of angular mode number (l) on the LG potential V(r). The latter represents positive LG profiles for the even values of angular mode number $l(= 0, 2)$ and the negative LG profiles are obtained for the odd values of angular mode number $l(= 1, 3)$, while fixing the azimuthal angle $\varphi = \pi$, the ion beam waist $\omega_0 = 3\lambda$, and $p = 0$. It is also seen that the peak of LG potential increases when the angular mode number is increased and the node points move toward a larger value of r. Figure 2.4 displays the effect of radial mode number $p(= 0, 1, 2, 3, 4)$ with fixed azimuthal angle $\varphi = \pi$ on the LG potential profiles. It is observed that at fixed $l = 1$, the number of node points are increased giving rise to significant modification in the LG potentials.

To study the LG potential profiles, we have used the following table to compute the Laguere polynomials and Laguerre-Gaussian functions with different quantum mode numbers l and p.

No.	Laguerre Gaussian polynomials	Laguerre Gaussian functions
1	$L_p^{\lvert l\rvert}(x) = e^{(x)}\frac{x^{-l}}{p!}\left[\frac{d^p}{dx^p}\left\{x^{l+p}e^{(-x)}\right\}\right]$	$F_{pl}(r,z) = \frac{1}{2\sqrt{\pi}}\left\{\frac{(l+p)!}{p!}\right\}^{1/2} x^{\lvert l\rvert} L_p^{\lvert l\rvert}(x)\, e^{(-x/2)}$
2	$L_0^0(x) = 1$	$F_{0,0}(r,z) = \frac{1}{2\sqrt{\pi}}\exp\left(-\frac{x}{2}\right)$
3	$L_1^0(x) = 1 - x$	$F_{1,0}(r,z) = \frac{1}{2\sqrt{\pi}}(1-x)\exp\left(-\frac{x}{2}\right)$
4	$L_2^0(x) = 1 - 2x + \frac{x^2}{2}$	$F_{2,0}(r,z) = \frac{1}{2\sqrt{\pi}}\left(1 - 2x + \frac{x^2}{2}\right)\exp\left(-\frac{x}{2}\right)$
5	$L_3^0(x) = 1 - 3x + \frac{3}{2}x^2 - \frac{1}{6}x^3$	$F_{3,0}(r,z) = \frac{1}{2\sqrt{\pi}}(1 - 3x + \frac{3}{2}x^2 - \frac{1}{6}x^3)\exp\left(-\frac{x}{2}\right)$
6	$L_4^0(x) = 1 - 3x + \frac{5}{2}x^2 - \frac{2}{3}x^3 + \frac{1}{24}x^4$	$F_{4,0}(r,z) = \frac{1}{2\sqrt{\pi}}\left(1 - 3x + \frac{5}{2}x^2 - \frac{2}{3}x^3 + \frac{1}{24}x^4\right)$ $\times \exp\left(-\frac{x}{2}\right)$
7	$L_0^1(x) = 1$	$F_{01}(r,z) = \frac{1}{2\sqrt{\pi}}(x)\exp\left(-\frac{x}{2}\right)$
8	$L_0^2(x) = 1$	$F_{02}(r,z) = \frac{\sqrt{2}}{2\sqrt{\pi}}\left(x^2\right)\exp\left(-\frac{x}{2}\right)$
9	$L_0^3(x) = 1$	$F_{03}(r,z) = \frac{\sqrt{3}}{2\sqrt{\pi}}\left(x^4\right)\exp\left(-\frac{x}{2}\right)$
10	$L_0^4(x) = 1$	$F_{04}(r,z) = \frac{1}{\sqrt{\pi}}(x^4)\exp\left(-\frac{x}{2}\right)$
11	$L_1^1(x) = 1$	$F_{11}(r,z) = \frac{\sqrt{2}}{2\sqrt{\pi}}x\,(1-x)\exp\left(-\frac{x}{2}\right)$
12	$L_2^1(x) = 3 - 3x + \frac{1}{2}x^2$	$F_{21}(r,z) = \frac{1}{2\sqrt{\pi}}\sqrt{3}x\left(3 - 3x + \frac{1}{2}x^2\right)\exp\left(-\frac{x}{2}\right)$
13	$L_3^1(x) = 4 - 6x + 2x^2 - \frac{1}{6}x^3$	$F_{31}(r,z) = \frac{1}{\sqrt{\pi}}x\left(4 - 6x + 2x^2 - \frac{1}{6}x^3\right)\exp\left(-\frac{x}{2}\right)$
14	$L_4^1(x) = 5 - 10x + 5x^2 - \frac{5}{6}x^3$ $+\frac{1}{24}x^4$	$F_{41}(r,z) = \frac{\sqrt{5}}{2\sqrt{\pi}}x\left(5 - 10x + 5x^2 - \frac{5}{6}x^3 + \frac{1}{24}x^4\right)$ $\times \exp\left(-\frac{x}{2}\right)$

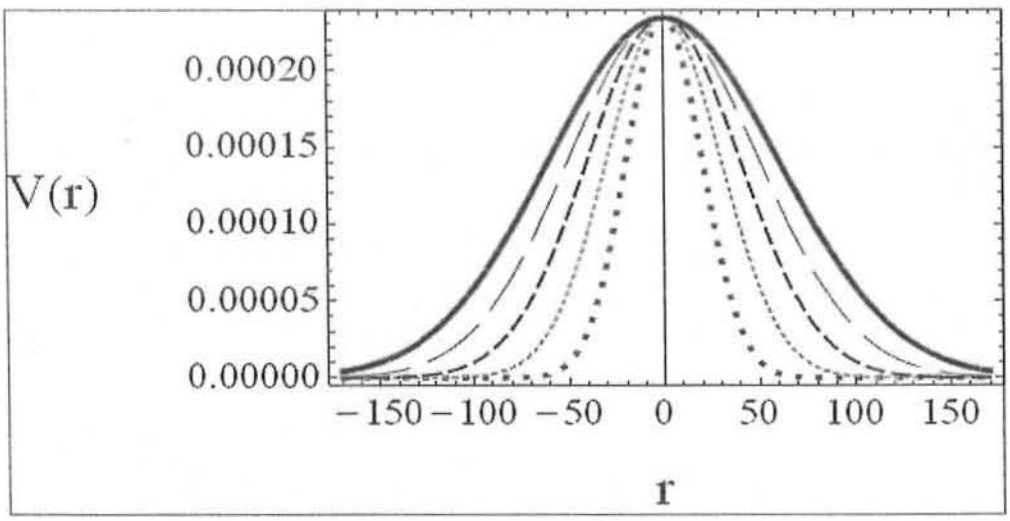

Figure 2-1: Shows LG potential profiles or a function of r for varying $\omega_0 = 2\lambda$ (square doted curve), $\omega_0 = 3\lambda$ (small doted curve), $\omega_0 = 4\lambda$ (small dashed curve), $\omega_0 = 5\lambda$ (long dashed curve), $\omega_0 = 6\lambda$ (solid curve) these are the pure Gaussian curves with fixed $l = 0 = p$.

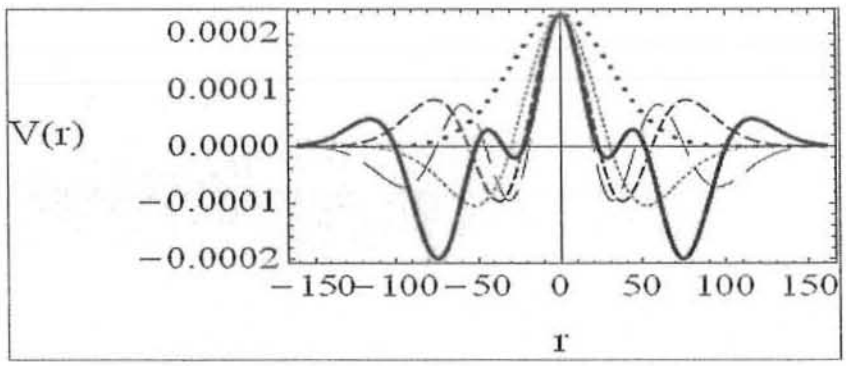

Figure 2-2: Shows the variation in the LG potential V(r) for varying radial mode number p=0 (square doted curve), p=1 (small doted curve), p=2 (small dashed curve), p=3 (long dashed curve) and p=4 (solid curve) with fixed angular mode number, l=0, and $\omega_0 = 3\lambda$, and $\lambda = 10$ cm^3

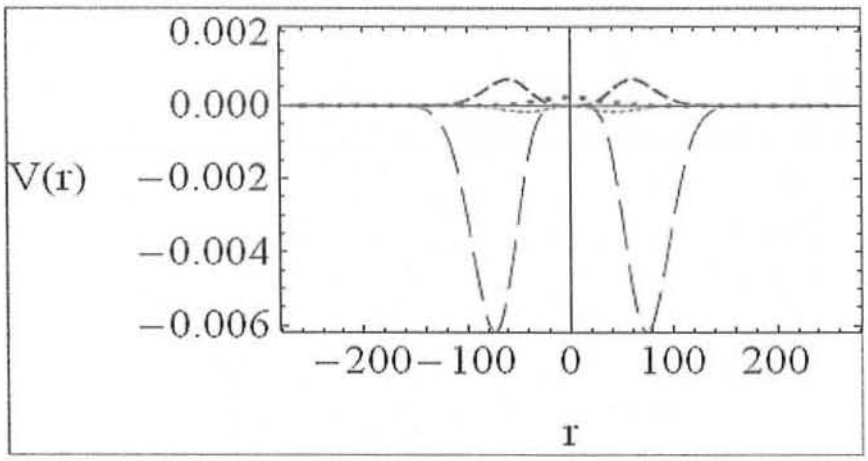

Figure 2-3: Shows that the LG potential V(r) for varying angular mode number $l = 0$ (square doted curve), $l = 1$ (small doted curve), $l = 2$ (small dashed curve), $l = 3$ (long dashed curve) and $l = 4$ (solid curve) with fixed radial mode number $p = 0$, the azimutal angle $\varphi = \pi$

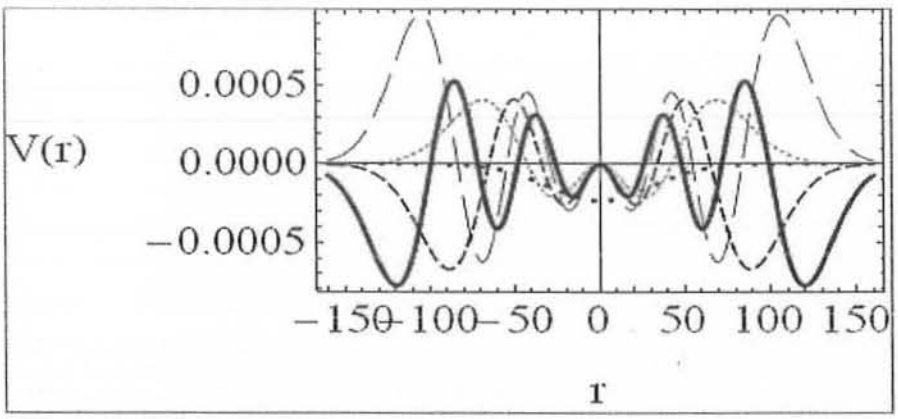

Figure 2-4: Shows the variation of LG potential profiles for fixed $l = 1$, and with changing, $p = 0$ (square doted curve), $p = 1$ (small doted curve), $p = 2$ (small dashed curve), $p = 3$ (long dashed curve), $p = 4$ (Solid curve), at a focal point for $t = 0$, $\varphi = \pi$, and $\omega_0 (= 3\lambda)$.

Chapter 3

Raman and Brillouin Backscattering of Light Beam Carrying OAM

3.1 Introduction

The exchange of angular momentum between the electrostatic and the electromagnetic waves has recently been studied in an unmagnetized collisionless plasma [42]. In this respect, Beth and Holbourn [39] computed experimentally the mechanical torque by exchange of angular momentum to a half wave plate. Allen et al. [45] theoretically investigated the orbital angular momentum of the Laguerre-Gaussian light beams. Mendonca et al. [52] computed the orbital angular momentum of plasmons in an unmagnetized plasma. Ayub et al. [56] extended the study of the orbital angular momentum for phonons. The exchange of angular momentum between electrostatic and electromagnetic waves has been explained in a plasma under the Brillouin and Raman backscattering processes. It is now established that [46] the angular momentum of electromagnetic radiations comprises of two distinct parts, one related to the polarization state due to transverse part of electromagnetic radiation or photon spin and the other is the orbital angular momentum (OAM) caused by the phase structure. We shall study the coupling of the light waves with the electrostatic modes like plasmons and phonons. For this purpose, we shall derive the nonlinear dispersion for light waves, electron waves and IA waves and we introduce the related concepts of photons, phonons and plasmons angular momentum states. These electrostatic and electromagnetic wave modes may be determined by the

solutions of the paraxial equations. Furthermore, solve these nonlinear equations for Laguerre-Gaussian mode solutions by coupling the incident and backscattered nonlinear equations in an unmagnetized collisionless uniform plasma. The spin effects for the electrostatic oscillations are not present, which means that their orbital angular momentum corresponds with their total angular momentum. When the electromagnetic and electrostatic waves nonlinearly interact with each other then the instability growth rates with OAM states are observed. Brillouin and Raman instabilities are famous in the application of laser fusion [47]. Raman backscattering is now distinguished as a dominant process for very high-intense laser plasma interactions in the reference of inertial confinement fusion (ICF) research [57]. The orbital angular momentum's dependence experimentally has been observed in Brillouin scattering of radio waves in ionosphere [69], which anticipates for a theoretical understanding. In all the ICF studies, the photon orbital angular momentum in specific and angular momentum in common have been orderly ignored.

3.2 Coupled Nonlinear Dispersion Relation for Electromagnetic Wave

First of all, in order to study electromagnetic waves in a plasma, we consider the following well-known Maxwell's equations, as

$$\nabla \times \mathbf{B} = \frac{4\pi}{c}\mathbf{J}_e + \frac{1}{c}\frac{\partial \mathbf{E}}{\partial t}, \tag{3.1}$$

$$\nabla \times \mathbf{E} = -\frac{1}{c}\frac{\partial \mathbf{B}}{\partial t}, \tag{3.2}$$

and

$$\mathbf{B} = \nabla \times \mathbf{A}, \tag{3.3}$$

where

$$\mathbf{J}_e = -\mathbf{n}_e e \mathbf{v}_e, \tag{3.4}$$

is the electron current density, c is the speed of light in vacuum and $\mathbf{A}$ is the vector potential.

Equation (3.1) may be expressed, as

$$-\nabla^2 \mathbf{A} = \frac{4\pi}{c}\mathbf{J}_e + \frac{1}{c}\frac{\partial \mathbf{E}}{\partial t}, \tag{3.5}$$

where we have assumed Coulomb gauge i.e. $\nabla \cdot \mathbf{A} = \mathbf{0}$. By using linear theory, we assume that $n_e = n_0 + \tilde{n}_1$ and $\mathbf{v}_e = \tilde{\mathbf{v}}_1$, n_0 is the electron density at equilibrium, $\tilde{n}_1$ is the electron density perturbation and $\tilde{\mathbf{v}}_1$ is the perturbed electric field velocity. Substituting these perturbations the current density gives

$$\mathbf{J}_e = -n_0 e\tilde{\mathbf{v}}_1 - \tilde{n}_1 e\tilde{\mathbf{v}}_1 \tag{3.6}$$

Putting Eq.(3.6) into Eq.(3.5), we get

$$-\nabla^2 \mathbf{A} = -\frac{4\pi}{c}n_0 e\tilde{\mathbf{v}}_1 - \frac{4\pi}{c}\tilde{n}_1 e\tilde{\mathbf{v}}_1 + \frac{1}{c}\frac{\partial \mathbf{E}}{\partial t}. \tag{3.7}$$

From (3.2) and (3.3) we express the electric field in terms of vector potential, as

$$\mathbf{E} = -\frac{1}{c}\frac{\partial \mathbf{A}}{\partial t}, \tag{3.8}$$

where the velocity gives

$$\tilde{\mathbf{v}}_1 = \frac{e\mathbf{A}}{m_e c} \tag{3.9}$$

Substituting Eq. (3.8) and Eq. (3.9) into Eq. (3.7), we get

$$\left(\partial_t^2 - c^2\nabla^2 + \omega_{pe}^2\right)\mathbf{A} = -\omega_{pe}^2 \frac{\tilde{n}_1}{n_0}\mathbf{A}, \tag{3.10}$$

where $\omega_{pe} = \left(4\pi n_0 e^2/m_e\right)^{1/2}$ is the electron plasma frequency, and m_e is the electron mass. Equation (3.10), shows the propagation of electromagnetic waves in an unmagnetized plasma. The term on the R.H.S represents the nonlinear contribution, while, the L.H.S gives linear terms. Considering the linear part and assuming a plane wave solution and $\omega_{pe} \to 0$, we obtain the usual dispersion relation of the electromagnetic waves as $\omega^2 = c^2k^2$.

3.3 Nonlinear Dispersion Relation for Plasmons (Langmuir waves)

The dynamics of the electron waves or plasmon mode is governed by the following equations

The continuity equation for electrons

$$\partial_t \tilde{n}_1 + n_0 \nabla \cdot \tilde{\mathbf{v}}_1 = 0 \tag{3.11}$$

The electron momentum equation,

$$(\partial_t + \tilde{\mathbf{v}}_1 \cdot \nabla)\, \tilde{\mathbf{v}}_1 = -\frac{e}{m_e}\mathbf{E} - \frac{k_B T_e}{m_e n_0}\nabla \tilde{n}_1. \tag{3.12}$$

The Poisson equation

$$\nabla \cdot \mathbf{E} = -4\pi e \tilde{n}_1 \tag{3.13}$$

Taking the divergence on both sides of Eq. (3.12), we obtain

$$\partial_t\, (\nabla \cdot \tilde{\mathbf{v}}_1) + \frac{1}{2}\nabla^2 \mid \tilde{\mathbf{v}}_1 \mid^2 = -\frac{e}{m_e}\nabla \cdot \mathbf{E} - \frac{k_B T_e}{m_e n_0}\nabla^2 \tilde{n}_1, \tag{3.14}$$

where we have used $\tilde{\mathbf{v}}_1 \nabla \cdot \tilde{\mathbf{v}}_1 = \frac{1}{2}\nabla^2 \mid \tilde{\mathbf{v}}_1 \mid^2$.

Now substituting the Poisson's equation, the continuity equation, and $\tilde{\mathbf{v}}_1 = e\mathbf{A}\ /m_e c$ into (3.14), a simplified equation is obtained

$$\left(\frac{\partial^2}{\partial t^2} - S_e^2 \nabla^2 + \omega_{pe}^2\right) \tilde{n}_1 = \frac{n_0 e^2}{2 m_e^2 c^2}\nabla^2 \mid \mathbf{A} \mid^2 \tag{3.15}$$

It is the nonlinear dispersion relation of the electron waves, $S_e = (k_B T_e / m_e)^{1/2}$, the electron thermal speed with electron temperature T_e. Right hand side shows a nonlinear contribution to the linear dispersion relation on the L.H.S. Equation (4.15) can be solved by using a plane wave solution while neglecting the nonlinear term to obtain $\omega^2 = \omega_{pe}^2 + S_e^2 k^2$, where $\omega(k)$ is the angular wave frequency (wave number) of the electron waves.

3.4 Paraxial Equations for Electromagnetic and Electron Plasma Waves

Let us now suppose that the Electromagnetic and Electrostatic waves are propagating along the z-axis and the solution to equations (3.10) and (3.15) are given by

$$\vec{A} = \sum_{j=1,2} \vec{A}_j \exp\left(ik_j z - i\omega_j t\right) + c.c., \tag{3.16}$$

and

$$\tilde{n}\left(\mathrm{r}, t\right) = \tilde{n}_1\left(\mathrm{r}, t\right) \exp\left(ik' z - i\omega' t\right) + c.c. \tag{3.17}$$

Here *c.c.* stands for complex conjugate, k_j and ω_j are the wavenumbers and the frequencies of two electromagnetic waves (the incident and scattered one). k' and ω' are the wavenumber and wave frequency of electron waves.

Supposing that $\tilde{n}_1$ and $\vec{A}_j$ are varying slowly on time and space scales and they are much larger than the corresponding periods and wave length. Decomposing the operator $\nabla = \nabla_\perp + \hat{z}\frac{\partial}{\partial z}$ and assuming the paraxial approximations viz. $\partial^2 \tilde{n}_1/\partial z^2 << 2ik_z \partial \tilde{n}_1/\partial z$ and $\partial_t^2 \tilde{n}_1 << 2i\omega' \partial_t \tilde{n}_1$, the wave equation (3.10) may be written into two coupled equations, as

$$D_1 \vec{A}_1 = \frac{\omega_{pe}^2 \tilde{n}_1}{n_0} \vec{A}_2, \tag{3.18}$$

and

$$D_2 \vec{A}_2 = \frac{\omega_{pe}^2 \tilde{n}_1^*}{n_0} \vec{A}_1, \tag{3.19}$$

where

$$D_1 = 2i\omega_1 \frac{\partial}{\partial t} + c^2\left(\nabla_\perp^2 + 2ik_1 \frac{\partial}{\partial z}\right), \qquad D_2 = 2i\omega_2 \frac{\partial}{\partial t} + c^2\left(\nabla_\perp^2 + 2ik_2 \frac{\partial}{\partial z}\right) \tag{3.20}$$

Similarly, the equation (4.15) can also be written in the form, as

$$D' \tilde{n}_1 = n_0 \frac{e^2 k'^2}{2m_e^2 c^2}\left(\vec{A}_1 \cdot \vec{A}_2^*\right), \tag{3.21}$$

where

$$D' = 2i\omega' \frac{\partial}{\partial t} + c^2 \left(\nabla_\perp^2 + 2ik' \frac{\partial}{\partial z} \right), \tag{3.22}$$

where we have assumed $j = 1, 2$, then the momentum and energy conservation give

$$k_1 = k_2 + k', \qquad and \qquad \omega_1 = \omega_2 + \omega' \tag{3.23}$$

The linear dispersion relations are satisfied for electrostatic and transverse modes, $k'^2 S_e^2 = (\omega'^2 - \omega_{pe}^2)$ and $k_j^2 c^2 = (\omega_j^2 - \omega_{pe}^2)$, respectively, and if $\omega' \simeq \omega_{pe}$, then as a result the incident wave frequency becomes twice of the value, i.e. $\omega_1 \geq 2\omega_{pe}$. It is also seen that, in order to make all these conditions well-matched with each other, we have to consider the two electromagnetic modes move in the opposite directions, with $k' > 0$ in case of electrostatic wave, with $k_1 > 0$, and $k_2 = - \mid k_2 \mid < 0$, for the incident and backscattered waves, respectively. For ignoring the coupling terms on the R.H.S, the linear approximation is obtained. The temporal dependence of the amplitudes $\tilde{n}_1$ and $\vec{A}_j$ will disappear and the linear equations may be converted into the pure paraxial equations, having the form,

$$\left(\nabla_\perp^2 + 2ik_j \frac{\partial}{\partial z} \right) \vec{A}_j = 0 \tag{3.24}$$

and

$$\left(\nabla_\perp^2 + 2ik'_z \frac{\partial}{\partial z} \right) \tilde{n}_1(\mathrm{r}) = 0 \tag{3.25}$$

Assuming the cylindrical coordinates $\vec{r} \equiv (r, \varphi, z)$, we express the paraxial solution of Eq. (3.24) as the linear combination of the Laguerre Gaussian modes,

$$\vec{A}_j(\mathrm{r}) = \vec{A}_{p_j l_j}(z) F_{p_j l_j}(r, z) \exp\left(i l_j \varphi\right) + c.c., \tag{3.26}$$

where $F_{p_j l_j}(r, z)$ are the Laguerre Gaussian functions which are defined by,

$$F_{pl}(r, z) = \left(\frac{1}{2\sqrt{\pi}} \right) \left\{ \frac{(l_j + p_j)!}{p_j!} \right\}^{\frac{1}{2}} X_j^{|l_j|} L_{p_j}^{|l_j|}(X_j) \tag{3.27}$$

The integers l_j, p_j denote the azimuthal and radial quantum numbers, and φ stands for the

azimuthal angle and $X_j = \frac{r^2}{\omega_j^2(z)}$, where $\omega_j(z)$ is the beam waist. Associated Laguerre polynomials can be defined as $L_{p_j}^{|l|}(X_j) = X_j^{-l_j}/p_j! \left[\frac{d^{p_j}}{dX^{p_j}}\left\{X^{l_j+p_j}\exp(-X_j)\right\}\right]\exp(X_j)$. The orthogonality relations of the Laguerre Gaussian modes can written as, $\int_0^\infty r dr F_{p_1,l_1}(r,z)F^*_{p_2,l_2}(r,z)$ $\times \int_0^{2\pi} d\varphi e^{i(l_1-l_2)\varphi} = \delta_{p_1,p_2}\delta_{l_1,l_2}$, where δ is the kronecker delta symbol. These solutions correspond to the definite photon OAM states described by azimuthal quantum numbers l_j. In the same way, we can say that the solutions for the Eq. (3.25) give a superposition of the plasmon angular momentum states, described by azimuthal and radial quantum numbers l' and p', respectively of the form, $F_{p'l'}(r,z)e^{il'\varphi}$, and the beam waist for both waves is considered to be the same, while the electrostatic waves have zero spin and angular momentum, no intrinsic angular momentum, because (in contrast to the transverse photons) plasmons have zero spin. Thus, angular momentum states of plasmons correspond with their total angular momentum states. Therefore, the electric field fluctuations involving with the plasmon states will stay purely electrostatic, while obeying the condition $\nabla \times \mathbf{E} = 0$. The solutions in the form $\mathbf{E}(\mathbf{r},t) = \mathbf{E}(\mathbf{r})\exp\left(ik'z - i\omega' t + il'\varphi\right)$, also indicate the angular and radial components of electric field. Thus, the solutions for the electron density fluctuations of LG modes can be expressed as,

$$\tilde{n}_1(r,\varphi,z) = \tilde{n}_{p'l'}(z)F_{p'l'}(r,z)\exp(il'\varphi + ik'z - i\omega' t) + c.c. \tag{3.28}$$

From Eqs. (3.18) - (3.21), we note to see that even in the form of LG modes they express the exchange of linear momentum as well as orbital angular momentum and exchange of energy, between longitudinal and two electromagnetic waves.

Now solve Eqs. (3.18), (3.19) and (3.21) by using Eqs. (3.26) and (3.28), respectively, as

$$2i\omega_1\frac{\partial}{\partial t}\vec{a}_1F_1^2 = \frac{\omega_{pe}^2}{n_0}\vec{a}_2n_1'F'F_1F_2e^{i(l'+l_2-l_1)\varphi}, \tag{3.29}$$

$$2i\omega_2\frac{\partial}{\partial t}\vec{a}_2F_2^2 = \frac{\omega_{pe}^2}{n_0}\vec{a}_1n_1^{*\prime}F^{*\prime}F_1F_2e^{i(-l'+l_1-l_2)\varphi}, \tag{3.30}$$

and

$$2i\omega'\frac{\partial}{\partial t}n'F'^2 = \frac{n_0e^2k'^2}{2m_e^2c^2}(\vec{a}_1\cdot\vec{a}_2^*)F'F_1F_2^*e^{i(l_1-l'-l_2)\varphi}, \tag{3.31}$$

where we have assumed that, $F_j = F_{p_jl_j}(r,z)$, $F' = F_{p'l'}(r,z)$, $\vec{a}_j = \vec{A}_{p_j,l_j}(z,t)$, $n' = n_{p'l'}(z,t)$.

Now integrating over φ on both sides Eqs. (3.29), (3.30) and (3.31), we obtain,

$$F_1^2 \partial_t \vec{a}_1 = -i \frac{\omega_{pe}^2 n'}{2 n_0 \omega_1} \vec{a}_2 F' F_1 F_2 \delta(l' + l_2 - l_1), \tag{3.32}$$

$$F_2^2 \partial_t \vec{a}_2 = -i \frac{\omega_{pe}^2 n^{*\prime}}{2 n_0 \omega_2} \vec{a}_1 F^{*\prime} F_1 F_2 \delta(-l' - l_2 + l_1), \tag{3.33}$$

and

$$F'^2 \partial_t n' = -i \frac{n_0 e^2 k'^2}{4 m_e^2 c^2 \omega'} (\vec{a}_1 \cdot \vec{a}_2^*) F' F_1 F_2^* \delta(-l' - l_2 + l_1) \tag{3.34}$$

Integrating these three equations over the radial coordinate r on both sides, we get

$$\partial_t \vec{a}_1 = -i c_1 n' \vec{a}_2, \tag{3.35}$$

$$\partial_t \vec{a}_2 = -i c_2 n^{*\prime} \vec{a}_1 \quad or \quad \partial_t \vec{a}_2^* = i c_2 n' \vec{a}_1^*, \tag{3.36}$$

and

$$\partial_t n' = -i c' (\vec{a}_1 \cdot \vec{a}_2^*), \tag{3.37}$$

where we have assumed that

$$c_j = \frac{\omega_{pe}^2}{2 n_0 \omega_j} R \qquad , \qquad c' = \frac{n_0 e^2 k'^2}{4 m_e^2 c^2 \omega'} R, \tag{3.38}$$

and

$$R \equiv R(z) \simeq \int_0^\infty F_1 F_2 F' r dr. \tag{3.39}$$

We have also used the following orthogonality conditions,

$$\int_0^\infty F_1^2 r dr \simeq 1, \ \int_0^\infty F_2^2 r dr \simeq 1, \ \int_0^\infty F'^2 r dr \simeq 1, \tag{3.40}$$

3.4.1 Growth Rates of Backscattered Electromagnetic and Plasmon Waves

In order to study, the stimulated Raman scattering by assuming the intense incident wave with amplitude $\vec{a}_1$ and to applying the parametric approximation $\partial \vec{a}_1 / \partial t \simeq 0$, we consider

the maximum coupling conditions corresponding to parallel polarization $\vec{a}_1 \parallel \vec{a}_2$. Then the remaining two equations can easily be solved to obtain the growth rates as,

$$\frac{\partial^2}{\partial t^2} n' = \gamma^2 n', \tag{3.41}$$

and

$$\frac{\partial^2}{\partial t^2} \vec{a}_2 = \gamma^2 \vec{a}_2, \tag{3.42}$$

where

$$\gamma = \omega_{pe}^2 \frac{ek'R}{2m_e\sqrt{\omega'\omega_2}} \mid \vec{a}_1 \mid \tag{3.43}$$

Equations (3.41) and (3.42) are the second order differential equations having unstable solutions as,

$$a_2(z,t) = a_2(z,0)e^{\gamma t} \text{ , and } n'(z,t) = n'(z,0)e^{\gamma t} \tag{3.44}$$

These equations indicate the incident wave of amplitude a_1 exciting the Langmuir waves with different angular momentum states. If we consider the plasmons carrying no angular momentum then following state $l_2 = -l_1$, will be the state of the backscattered wave, but it has been observed that the $l_2 \neq -l_1$ is the state of backscattered signal, which indicates that the plasmons are moving in the medium with non-zero AM states, then the Raman backscattering can be used as an influential diagnostic method to observe the internal plasma vorticity. We suppose now a motivating cases in which we use two counter propagating electromagnetic waves from outside to excite the plasmons to well-defined angular momentum states. Going back to Eqs. (3.35), (3.36) and (4.37) the amplitude of the perturbed plasmon state can be found, as a function of $a_2(z,0)$. We assume $\mid a_1 \mid \gg \mid a_2 \mid$ and apply the parametric approximation $\partial a_1/\partial t \simeq 0$, for parallel polarization, Eqs. (3.35), (3.36) and (3.37) can be reduced to the following form,

$$\partial_t \vec{a}_2^* = ic_2 n' \vec{a}_1^* e^{-i\Delta\omega t}, \tag{3.45}$$

and

$$\partial_t n' = -ic'(\vec{a}_1 \cdot \vec{a}_2^*) e^{i\Delta\omega t}, \tag{3.46}$$

where a finite frequency mismatch $\Delta\omega = \omega_1 - \omega_2 - \omega\prime$ has been introduced, as the two electromagnetic wave modes have been executed from the outside, therefore the waves are essentially not in a definite matching conditions. So, we may write

$$\partial_t^2 n' = \gamma^2 n' + i\Delta\omega\partial_t n', \tag{3.47}$$

and similarly,

$$\partial_t^2 \vec{a}_2^* = \gamma^2 \vec{a}_2^* - i\Delta\omega\partial_t \vec{a}_2^*, \tag{3.48}$$

where, $c'c_2 \mid a_1 \mid^2 = \gamma^2$. Now solve these two equations with the initial conditions such that $n'(z,0) = 0$, and for arbitrary $a_2(z,0)$, we can write the solutions in the following form

$$\vec{a}_2^*(z,t) = \vec{a}_2^*(z,0)\cosh(gt)e^{(-i\Delta\omega t/2)}, \tag{3.49}$$

or

$$\vec{a}_2(z,t) = \vec{a}_2(z,0)\cosh(gt)e^{(i\Delta\omega t/2)} \tag{3.50}$$

and $g = \left[\gamma^2 - (\Delta\omega/2)\right]^{1/2}$. Now putting the value of $\vec{a}_2^*(z,t)$ from Eq. (3.49) into Eq. (3.46) and then integrating w.r.t. time, the final result for density perturbation becomes

$$n'(z,t) = -i\frac{c'a_1}{g}a_2(z,0)\sinh(gt)e^{(i\Delta\omega t/2)} \tag{3.51}$$

These two Eqs. (3.50) and (3.51) explain the excitation of backscattered plasmon angular momentum state which is characterized by the azimuthal number $l' = l_1 - l_2$, and the backscattered growth signal with OAM state l_2. Growth rates are depended on the axial position z, which means that very rapidly the axial profile of both the electrostatic modes and excited backscattered will diverge from its linear solution, but the radial beam profile will not be changed.

3.5 Brillouin Instability or Ion-Acoustic Wave

Here, we consider the dynamics of ion-acoustic waves (phonons) and derive a nonlinear equation for phonons. For this purpose, we consider the momentum equations as

$$\frac{\partial \mathbf{v}_{e1}}{\partial t} + \mathbf{v}_{e1} \cdot \nabla \mathbf{v}_{e1} = -\frac{e}{m_e}\mathbf{E} - \frac{k_B T_e}{m_e n_{e0}} \nabla n_{e1} \tag{3.52}$$

Taking the $\nabla\cdot$ on the both sides and assuming inertialess electrons compared to ions so that we obtain

$$e\nabla \cdot \mathbf{E} = -m_e \nabla^2 \mid \mathbf{v}_{e1} \mid^2 - \frac{k_B T_e}{n_{e0}} \nabla^2 n_{e1}. \tag{3.53}$$

The linearized momentum equation for cold ions is given by

$$\frac{\partial \mathbf{v}_{i1}}{\partial t} = \frac{Ze}{M}\mathbf{E} \tag{3.54}$$

The linearized continuity equation for ions,

$$\frac{\partial n_{i1}}{\partial t} = -n_{i0} \nabla \cdot \mathbf{v}_{i1}, \tag{3.55}$$

Taking the time and space derivative of equations (3.55) and (3.54), respectively as

$$\frac{\partial^2 n_{i1}}{\partial t^2} = -n_{i0} \frac{\partial \left(\nabla \cdot \mathbf{v}_{i1}\right)}{\partial t}, \tag{3.56}$$

and

$$\frac{\partial \left(\nabla \cdot \mathbf{v}_{i1}\right)}{\partial t} = \frac{Ze}{M} \nabla \cdot \mathbf{E} \tag{3.57}$$

Combining Eq. (3.56) and (3.57), we may write

$$\frac{\partial^2 n_{i1}}{\partial t^2} = -n_{i0} \frac{Ze}{M} \nabla \cdot \mathbf{E}, \tag{3.58}$$

where Z is the charge number and M is the mass of ion. Substituting Eq. (3.53) into the Eq. (3.58), we get

$$\frac{\partial^2 n_{i1}}{\partial t^2} = n_{i0} \frac{Z}{M} \left(m_e \nabla^2 \mid \mathbf{v}_{e1} \mid^2 + \frac{k_B T_e}{n_{e0}} \nabla^2 n_{e1} \right) \tag{3.59}$$

As we also know that $\mid \mathbf{v}_{e1} \mid^2 = e^2 \mid \mathbf{A} \mid^2 / m_e^2$, $Zn_{i1} = n_{e1}$, and $Zn_{i0} = n_{e0}$ at equilibrium. Substituting these values in Eq. (3.59), the final result gives

$$\left(\frac{\partial^2}{\partial t^2} - C_s^2 \nabla^2\right) n_{i1} = \frac{Z n_{i0} e^2}{m_e M} \nabla^2 \mid \mathbf{A} \mid^2 \tag{3.60}$$

This is a nonlinear dispersion relation for the phonons, where $C_s = (Zk_B T_e/M)^{1/2}$ is the ion-acoustic speed. Now considering the solution for ion-acoustic oscillations, as

$$\tilde{n}_{i1}(\mathbf{r}, t) = n_{i1}(\mathbf{r}) \exp(ik'z - i\omega' t) + c.c., \tag{3.61}$$

and for electromagnetic wave equation (3.10), as

$$\vec{A}(\mathbf{r}, t) = \sum_{j=1,2} \vec{A}_j(\mathbf{r}) \exp(ik_j z - i\omega_j t) + c.c. \tag{3.62}$$

Applying the same procedure as done in case of plasmons, we solve Eq. (3.60), as

$$\left[2i\omega' \frac{\partial}{\partial t} + C_s^2 \left(\nabla_\perp^2 + 2ik' \frac{\partial}{\partial z}\right)\right] \tilde{n}_{i1} = \frac{Z n_{i0} e^2 k'^2}{m_e M} (\vec{A}_1 \cdot \vec{A}_2^*), \tag{3.63}$$

or

$$D' \, \tilde{n}_{i1} = n_{i0} \frac{Z e^2 k'^2}{mM} (\vec{A}_1 \cdot \vec{A}_2^*) \tag{3.64}$$

where

$$D' = 2i\omega' \frac{\partial}{\partial t} + C_s^2 \left(\nabla_\perp^2 + 2ik' \frac{\partial}{\partial z}\right) \tag{3.65}$$

The differential operator D' is the same as for the electron (plasmon) wave, but now the electron thermal speed S_e is replaced by the phonon's acoustic speed C_s. Now the parallel wavenumber k' satisfies the ion-acoustic dispersion relation as, $k'C_s = \omega'$ by applying the linear approximation, the electrostatic paraxial equation is obtained

$$\left(\nabla_\perp^2 + 2ik_z' \frac{\partial}{\partial z}\right) \tilde{n}_{i1}(\mathbf{r}) = 0 \tag{3.66}$$

This equation describes the angular momentum states for the ion-acoustic waves, similar to

those of plasmons, and its solution can be defined as,

$$\tilde{n}_{i1}(r,\varphi,z) = \tilde{n}_{p'l'}(z)F_{p'l'}(r,z)\exp(il'\varphi + ik'z - i\omega' t) + c.c \tag{3.67}$$

Using these solutions into the nonlinear phonons Eq. (3.60), the time dependent phonon amplitude similar to the plasmon case is obtained as,

$$\frac{\partial n'}{\partial t} = -iC_B a_1 a_2^*, \tag{3.68}$$

where

$$C_B = \frac{Zn_{i0}e^2k'}{m_e M C_s} R \tag{3.69}$$

Equation (3.68) leads to the stimulated Brillouin backscattering solutions with a growth rate in the following form

$$\frac{\partial^2}{\partial t^2} n' = \gamma_s^2 n', \tag{3.70}$$

with

$$\gamma_s = C_B C_2 \mid \vec{a}_1 \mid^2 \tag{3.71}$$

All those qualitative properties are repeated here which we have discussed for the Raman backscattering process. Thus, we have studied stimulated Raman and Brillouin backscattering of electromagnetic waves in an unmagnetized collisionless plasma involving OAM states.

3.6 Summary

In this Chapter, we have studied the coupling of the light waves with electrostatic modes like plasmons and phonons. First, we have derived the nonlinear dispersions of the Langmuir and IA waves and introduced the concepts of phonon and plasmon angular momentum states. The electrostatic wave modes are found by the solutions of the paraxial equations, similar to those expressing the electromagnetic wave beams close to the focal region. We have solved these nonlinear equations for Laguerre-Gaussian mode solutions by coupling the incident and backscattered nonlinear equations in the collisionless uniform plasma. Finally, the corresponding growth rates are determined by applying the parametric approximation. An additional

rule has been added for nonlinear wave interaction, related with the conservation of angular momentum. Specially, we have shown that by using two counter propagating electromagnetic waves with well-defined OAM, we can excite the definite states of non-zero phonon and plasmon angular momentum. The experimental confirmation of this theoretical model could be important to study basic plasma physics.

Chapter 4

Electron-Acoustic Wave with Orbital Angular Momentum

4.1 Introduction

Numerous investigations [58, 59, 60, 61, 62, 63] have been carried out to investigate the existence of two distinct groups of electrons, that are, the cold and hot electrons found in space and laboratory plasmas. The hot electrons can be of the energy in the range $(10-50)\ keV$ (kilo electron volt) and the cold electrons may be of the energy $(0.1-1)\ keV$ in laser produced plasmas [58], when the intensity of the laser exceeds the value $I \sim 10^{14} W/cm^2$ for Neodymimum-glass laser and $I \sim 10^{12} W/cm^2$ for CO_2 laser. Such a plasma is called two-temperature electron plasma, which supports the electron-acoustic (EA) waves and their properties are extensively investigated [64, 65, 66]. In the EA wave, the restoring force comes from the Boltzmann distributed hot electrons and the mass of the cold electrons provides inertia to maintain the wave. The frequency of the EA wave is larger than the ion plasma frequency while the phase velocity lies between the thermal speed of the hot and cold electrons i.e. $S_c << \omega/k << S_h$. It is also found that the phase velocity of EA wave is unusually small in comparison with the Langmuir waves. The EA mode is frequently found in space plasma (bow shock [70, 71], polar regions of the Earth's ionosphere [72, 73], solar corona [74] and the dayside cups region [75]). About two decades ago, Allen et al. [32] explained the orbital angular momentum (OAM) of the photons attributed to Laguerre-Gaussian laser beams. Mendonca et al. [46]

investigated the electron plasma waves carrying OAM in an unmagnetized uniform plasma and calculated the energy flux and electric field components suggesting an approximate solution for the electrostatic potential problem. Latter, Ayub et al. [56] extended the work for phonons or ion-acoustic waves and computed OAM states associating with the phonon modes.

In the following, we shall derive the OAM involving the EA modes in a two-temperature electron plasma. We will also present an approximate solution to the potential problem under the paraxial approximation.

4.2 Dispersion Relation of Electron-Acoustic Waves

To study the dispersion relation of the electron-acoustic (EA) wave, we consider a two-temperature electron plasma containing the inertial cold electrons, and massless Boltzmann distributed hot electrons with static ions. We shall be actually interested to study the orbital angular momentum states associated with EA modes. At equilibrium, the charge-neutrality condition demands $n_{i0} = n_{c0} + n_{h0}$, where n_{c0} (n_{h0}) is the cold electron (hot electron) unperturbed density.

The dynamics of the EA wave can be studied by employing the continuity equation

$$\frac{\partial n_{c1}}{\partial t} + n_{c0}\left(\nabla \cdot \mathbf{v}_{c1}\right) = 0, \tag{4.1}$$

the momentum equation

$$\frac{\partial}{\partial t}\mathbf{v}_{c1} = \frac{-e\mathbf{E}}{m_c}, \qquad \mathbf{E} = -\nabla V, \tag{4.2}$$

and the Poisson equation

$$\nabla \cdot \mathbf{E} = 4\pi e(-n_{c1} - n_{h1} + n_{i0}), \tag{4.3}$$

where the hot electron density perturbations obey the Boltzmann distribution

$$n_{h1} \simeq n_{h0}\frac{eV}{k_B T_h} \tag{4.4}$$

The electrostatic potential is denoted by $V(\mathbf{r}, t)$. Equation (4.4) can be derived when the electro-

static force is balanced with the pressure force in the momentum equation of hot electrons. $\mathbf{v}_{c1}$ stands for the cold electron fluid velocity, $n_{h1}(\ll n_{h0})$ the perturbed hot-electron density with equilibrium value n_{h0}, while $n_{c1}(\ll n_{c0})$ is the perturbed (unperturbed) cold-electron number density perturbation. T_h is the hot-electron temperature. Following the procedure as described in Chapter 2, we first take the time derivative of Eq. (4.1) to obtain

$$\frac{\partial}{\partial t}\nabla \cdot \mathbf{v}_{c1} = -\frac{1}{n_{c0}}\frac{\partial^2 n_{c1}}{\partial^2 t}, \tag{4.5}$$

and the divergence of the momentum equation gives

$$\frac{\partial}{\partial t}\nabla \cdot \mathbf{v}_{c1} = \frac{e}{m_e}\nabla^2 V \tag{4.6}$$

Combining Eqs. (4.5) and (4.6), we get

$$\frac{\partial^2}{\partial t^2} n_{c1} = -\frac{e}{m_c} n_{c0}\nabla^2 V \tag{4.7}$$

Putting Eq. (4.4) into Eq. (4.3), we obtain the electrostatic potential in terms of n_{c1} is written as

$$\left(1 - \nabla^2 \lambda_{Dh}^2\right) V = -4\pi e n_{c1} \lambda_{Dh}^2, \tag{4.8}$$

where $\lambda_{Dh} = \left(k_B T_h / 4\pi n_{h0} e^2\right)^{1/2}$, the hot electron Debye length. For long wave length limit [67], we assume $\nabla^2 \lambda_{Dh}^2 \ll 1$ and eventually Eq. (4.8) may be reduced to

$$V = -4\pi e n_{c1} \lambda_{Dh}^2. \tag{4.9}$$

Now combining Eq. (4.9) and Eq. (4.7), the linear dispersion relation of the EA waves is obtained

$$\left(\frac{\partial^2}{\partial t^2} - C_e^2 \nabla^2\right) n_{c1} = 0 \tag{4.10}$$

By using a plane wave solution of the form $n_{c1} = n_{c0} e^{i(\mathbf{k}.\mathbf{r} - \omega t)}$, one may write (4.10) in the following form

$$\omega = C_e k_z, \tag{4.11}$$

where ω (k_z) is the angular wave frequency (longitudinal wave number) of the electron-acoustic wave $C_e = \omega_{pc}\lambda_{Dh} \equiv \left(\frac{n_{c0}}{n_{h0}}\frac{k_B T_h}{m_e}\right)^{1/2}$ is the electron-acoustic speed and $\omega_{pc} = \left(4\pi n_{c0}e^2/m_c\right)^{1/2}$ stands for the cold electron plasma frequency. It is important to note that the electron-acoustic speed is significantly modified by the ratio of the cold electron number density and hot electron temperature.

4.3 Paraxial Equation for EA Waves

The usual plane wave solution does not carry orbital angular momentum and therefore we consider a beam type solution in order to derive the paraxial equation for the EA waves as given by

$$n_{c1}(\mathbf{r},t) = n_{c0}(\mathbf{r})\exp\left(ik_z z - i\omega t\right). \tag{4.12}$$

Here $n_{c0}(\mathbf{r})$ denotes the amplitude in the spatial coordinates varying slowly. Using Eq. (4.12) into (4.10), the wave equation becomes

$$\left(\frac{\partial^2}{\partial t^2} - C_e^2\nabla^2\right) n_{c0}(\mathbf{r})\exp\left(ik_z z - i\omega t\right) = 0, \tag{4.13}$$

where k_z ($= \omega/C_e$). Expressing the operator $\boldsymbol{\nabla} = \boldsymbol{\nabla}_\perp + \hat{\mathbf{z}}\partial/\partial z$ and using the paraxial approximation $\left\{viz. \frac{\partial^2}{\partial z^2}n_{c0}(\mathbf{r}) << 2ik_z\frac{\partial}{\partial z}n_{c0}(\mathbf{r})\right\}$, one can derive a paraxial equation for EA waves as

$$\left(2ik_z\frac{\partial}{\partial z} + \nabla_\perp^2\right) n_{c0}(\mathbf{r}) = 0, \tag{4.14}$$

where the solution of the above equation may be written in terms of LG functions as

$$\tilde{n}_{c0}(r,\varphi,z) = \tilde{n}_{pl}(z)F_{pl}(r,z)\exp(il\varphi + ikz - i\omega t), \tag{4.15}$$

where $\tilde{n}_{pl}(z) = \tilde{N}_{c0}F_{pl}(r,z)$, $\tilde{N}_{c0}$ is the amplitude of the cold electron density perturbations, $F_{pl}(r,z) = \frac{1}{2\sqrt{\pi}}\left\{\frac{(l+p)!}{p!}\right\}^{1/2} X^{|l|}L_p^{|l|}\exp\left(-X/2\right)$ are the LG functions with $X = r^2/\omega^2(z)$, $\omega(z)$ is the EA beam waist, and φ denotes the azimuthal angle. l and p are the azimuthal and radial mode numbers and $L_p^{|l|}$ is the Laguerre polynomials.

4.4 Electrostatic Potential Problem

In order to characterize the EA waves, we solve the electrostatic potential problem in uniform plasma consisting of Boltzmann distributed hot electrons, the inertial cold electrons with stationary ions. Thus, the electrostatic potential in terms of density perturbations can be described by the Poisson equation, as

$$\nabla^2 V(\mathbf{r},t) = 4\pi e(n_{h1} + n_{c1}), \tag{4.16}$$

A direct solution to Eq. (4.16) is a difficult task and here we will be interested into an approximate solution by using a paraxial approximation. The LG potential $V(\mathbf{r},t)$ can be expressed by the following relation

$$V(\mathbf{r},t) = V_{pl}(r,z)e^{(il\varphi + ik_z z - i\omega t)}. \tag{4.17}$$

Substituting Eqs. (4.4) and (4.17) into Eq. (4.16), we arrive at

$$\left\{\left(\nabla_\perp^2 + 2ik_z\frac{\partial}{\partial z}\right) - k_z^2 - \frac{1}{\lambda_{Dh}^2}\right\} V(\mathbf{r},t) = 4\pi e n_{c1} \tag{4.18}$$

Equation (4.18) can be solved by satisfying the paraxial approximation, similar to Eq. (4.14) i.e. $\left(\nabla_\perp^2 + 2ik_z\frac{\partial}{\partial z}\right) V(\mathbf{r},t) = 0$. Hence the amplitude of the electrostatic potential from (4.17) may be expressed as $V_{pl}(r,z) = V_{c0}F_{pl}(r,z)$.

Thus, the LG potential involving the EA wave becomes

$$V(\mathbf{r},t) = V_{c0}F_{pl}(r,z)e^{(il\varphi + ik_z z - i\omega t)}, \tag{4.19}$$

and (4.18) may reduce to

$$V(\mathbf{r},t) = -4\pi e n_{c1}\left(\frac{\lambda_{Dh}^2}{1 + k_z^2\lambda_{Dh}^2}\right). \tag{4.20}$$

Note that the LG potential becomes negative in contrast to phonon case [56]. The amplitude involving LG potential perturbations in the presence of LG density perturbations, can be obtained as

$$V_{c0} = -4\pi e\frac{\lambda_{Dh}^2\tilde{N}_{c0}}{1 + k_z^2\lambda_{Dh}^2} \tag{4.21}$$

See that the amplitude of the LG potential is significantly modified due the presence of Boltz-

mann distributed hot electrons through the hot electron Debye shielding length, the EA wave number and the cold electron density perturbations.

Now using the relation $E(\mathbf{r},t) = -\nabla V$, we can find the LG electric field components in cylindrical coordinates (r,φ,z) as

$$\begin{aligned} E_r &= -\frac{V}{F_{pl}}\frac{\partial F_{pl}}{\partial r} \\ E_\varphi &= -i\frac{lV}{r} \\ E_z &= -\left(ik_z + \frac{1}{F_{pl}}\frac{\partial F_{pl}}{\partial r}\right)V \end{aligned} \tag{4.22}$$

However, the electric field can also be expressed in the usual way as $\mathbf{E} \equiv -i\mathbf{k}_{ef}V(\mathbf{r},t)$, where the effective wave vector is given as $\mathbf{k}_{ef} = -\frac{i}{F_{pl}}\frac{\partial F_{pl}}{\partial r}\hat{\mathbf{e}}_r + \frac{l}{r}\hat{\mathbf{e}}_\varphi + \left\{k_z - \frac{i}{F_{pl}}\frac{\partial F_{pl}}{\partial r}\right\}\hat{\mathbf{e}}_z$. Thus, we conclude that the electric field components are significantly affected by the EA beam waist through LG mode structure and the hot electron shielding length as well as the cold electron density fluctuations. It is also worth mentioning here that the electric field lines for the EA waves are in the form of helical structure with radial and azimuthal mode numbers as are absent in the plane wave solutions showing straight lines for the electric field.

4.5 Energy Flux and OAM for EA Waves

When an electron-acoustic wave propagates in an unmagnetized collisionless uniform plasma, it carries a finite amount of orbital angular momentum. The energy density for LG EA mode can be calculated by taking into account the dispersive properties of the plasma medium, as

$$W_{ea} = \frac{\mid E \mid^2}{8\pi}\frac{\partial}{\partial\omega}(\epsilon\omega), \tag{4.23}$$

where the dielectric constant for EA mode is given by

$$\epsilon(\omega,k_z) = 1 + \frac{1}{\lambda_{Dh}^2 k_z^2} - \frac{\omega_{pc}^2}{\omega^2 - k_z^2 S_c^2}. \tag{4.24}$$

density

The energy flux for EA mode can be defined [52] as $\mathbf{T}_{ea} = W_{ea}v_g\hat{\mathbf{e}}_{ef}$, where $\hat{\mathbf{e}}_{ef}\,(=\mathbf{k}_{ef}/\mid k_{ef}\mid)$ is the effective unit vector and v_g is the group velocity of the EA mode.

One may simplify energy density expression further as

$$W_{ea} = \frac{\mid E \mid^2}{8\pi}\left\{1 + \frac{1}{\lambda_{Dh}^2 k_z^2} + \omega_{pc}^2 \frac{\omega^2 + k_z^2 S_c^2}{(\omega^2 - k_z^2 S_c^2)^2}\right\}. \tag{4.25}$$

The energy density can be written in terms of LG potential by writing

$$\mid E \mid^2 = \mathbf{E}\cdot\mathbf{E}^* \equiv k_{ef}^2 \mid V \mid^2, \tag{4.26}$$

as

$$\mathbf{M(r)} = \mathbf{r}\times < \mathbf{P}_{ea} >, \tag{4.27}$$

where

$$< \mathbf{P}_{ea} > = \frac{< \mathbf{T}_{ea} >}{v_g^2} \equiv \frac{< W_{ea} > \hat{\mathbf{e}}_{ef}}{v_g} \tag{4.28}$$

Using Eq. (4.25) into the (4.28), we obtain

$$< \mathbf{P}_{ea} > \equiv \frac{k_{ef}^2 <\mid V \mid^2>}{8\pi v_g}\left[1 + \frac{1}{\lambda_{Dh}^2 k_z^2} + \omega_{pc}^2 \frac{\omega^2 + k_z^2 S_c^2}{(\omega^2 - k_z^2 S_c^2)^2}\right]\hat{\mathbf{e}}_{ef}. \tag{4.29}$$

By employing Eq. (4.29) into Eq. (4.27) and doing some straightforward algebra, we get

$$\begin{aligned}\mathbf{M(r)} &= \frac{\mid k_{ef} \mid <\mid V \mid^2>}{8\pi v_g}\left[-\frac{l r_{\parallel}}{r}\hat{\mathbf{e}}_r - \left\{\frac{i r_{\parallel}}{F_{pl}}\frac{\partial F_{pl}}{\partial r} + r k_z - \frac{ir}{F_{pl}}\frac{\partial F_{pl}}{\partial z}\right\}\hat{\mathbf{e}}_{\varphi} + l\hat{\mathbf{e}}_z\right] \\ &\times\left[1 + \frac{1}{\lambda_{Dh}^2 k_z^2} + \omega_{pc}^2 \frac{\omega^2 + k_z^2 S_c^2}{(\omega^2 - k_z^2 S_c^2)^2}\right]\end{aligned} \tag{4.30}$$

The angular momentum density of EA beam along the axial direction [53] can be expressed as

$$M_z = l\frac{\mid k_{ef} \mid <\mid V \mid^2>}{8\pi v_g}\left\{1 + \frac{1}{\lambda_{Dh}^2 k_z^2} + \omega_{pc}^2 \frac{\omega^2 + k_z^2 S_c^2}{(\omega^2 - k_z^2 S_c^2)^2}\right\} \tag{4.31}$$

Note that M_z depends not only on the square of magnitude of Laguerre Gaussian potential but also the inverse of the group velocity of the EA wave. Equation (4.31) is now significantly modified by the dielectric constant of the EA wave. For assuming that angular mode number $l = 0$, which implies that $M_z = 0$, leading to the lowest order mode or a pure Gaussian mode

with no OAM. However, for higher order modes i.e. $l \neq 0$, a finite amount of OAM associated with the EA waves can easily be investigated. Similarly, equation (4.19) through (4.21) also concludes that the amplitude of the negative LG potential profiles caused by the EA mode is strongly modified due to the cold-electron density perturbations and wave number k_z carrying the finite amount of OAM.

4.6 Numerical Results and Discussion for EA Modes

In this section, we have numerically plotted the LG potential V(r) associated with the EA mode as a function of "r", we have also chosen some appropriate numerical values from the laboratory two-temperature electron plasma [68], such as, the hot electron temperature $T_h \simeq 2.1eV$ and the cold electron temperature $T_c \simeq 0.7eV$, the hot electron density $n_h \simeq 2 \times 10^7 cm^{-3}$ and the cold electron density $n_c \simeq 6 \times 10^7 cm^{-3}$. By using these parameters, we can compute the ion number density $n_{i0} = 8 \times 10^7 cm^{-3}$, the wave number $k_z = 8.788\ cm$, and the hot electron Debye shielding length $\lambda_{Dh}^2 = 1.4506 \times 10^{-3} cm$. We also assume that the cold-electron density perturbation viz. $\tilde{N}_0/n_{c0} \sim 0.1$, which makes the amplitude of LG potential to be $\tilde{V}_{c0} \sim -5.18752 \times 10^{-5}\ V$ for the EA beam waist $\omega_0 = 3\lambda$, where $\lambda \sim 0.7149\ cm$. Figure 4.1 shows the variation of LG potential involving EA wave at a focal point for t=0. For changing the EA beam waist $\omega_0 = 2\lambda, 3\lambda, 4\lambda, 5\lambda, 6\lambda$ with fixed $l = 0 = p$, the pure Gaussian curves are obtained, the width of the LG profiles increases while the amplitude remains constant. However, the behavior of the EA wave is different from the IA wave. Non-Gaussian profiles of LG potential are obtained for $l = 0$ and $p \neq 0$, as can be seen in Fig. 4.2. It is examined that the number of nodes on both sides increases for the increase of p value and hence the LG potential amplitude remains almost constant but the width decreases with increasing p. Figure 4.3 exhibits the effect of angular mode number (l) on the LG potential V(r). The latter becomes negative for the variation of even values of angular mode number $l(= 0, 2)$ and becomes positive for odd values $l(= 1, 3)$ with $\omega_0 = 3\lambda$, the azimuthal angle $\varphi = \pi$, and $p = 0$. It is observed that the strength of LG potential increases when the angular mode number is increased. Figure 4.4 demonstrate the effect of the radial mode number $p(= 0, 1, 2, 3, 4)$ at fixed $l = 1, \omega_0 = 3\lambda$, and $\varphi = \pi$. Note that the number of nodes and the strength of the LG potential increase with

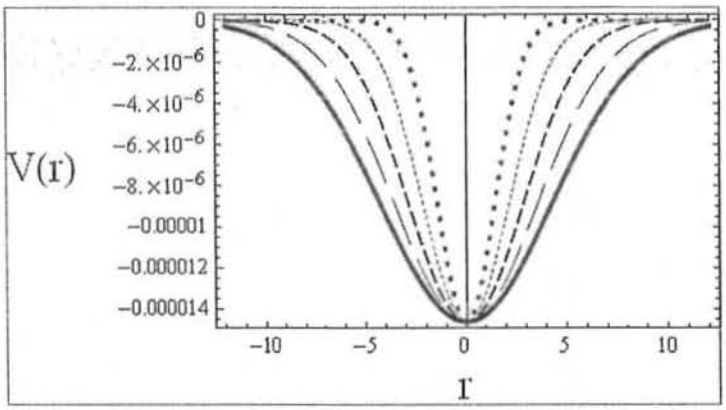

Figure 4-1: Shows LG potential profiles or a function of r for varying $\omega_0 = 2\lambda$ (square doted curve), $\omega_0 = 3\lambda$ (small doted curve), $\omega_0 = 4\lambda$ (small dashed curve), $\omega_0 = 5\lambda$ (long dashed curve), $\omega_0 = 6\lambda$ (solid curve) these are the pure Gaussian curves with fixed $l = 0 = p$.

increasing p. However, the behavior of the potential associated with EA wave profiles is seen opposite to the potential involving phonons [56].

4.7 Summary

To summarize, we have studied the two-temperature electron plasma which is composed of hot electrons, cold electrons, and positive ions. The hot electrons are assumed to follow the Boltzmann distribution while the cold electrons as mobile with a background of stationary ions. We have derived a linear dispersion relation for the electron-acoustic (EA) waves by using the Laguerre Gaussian solutions giving rise to an orbital angular momentum, instead of plane wave solution. Furthermore, the electrostatic potential problem is solved by employing the Laguerre Gaussian beam solutions and the electric field components have been computed in terms of LG potential suggesting that the helical field structures are formed. Similarly, the energy density and orbital angular momentum of the EA modes have been determined by considering the dispersive plasma medium. The numerical results for the LG potential involving the EA modes have been discussed, which are of significant importance for understanding the EA waves with OAM states in the context of laser produced and space plasmas.

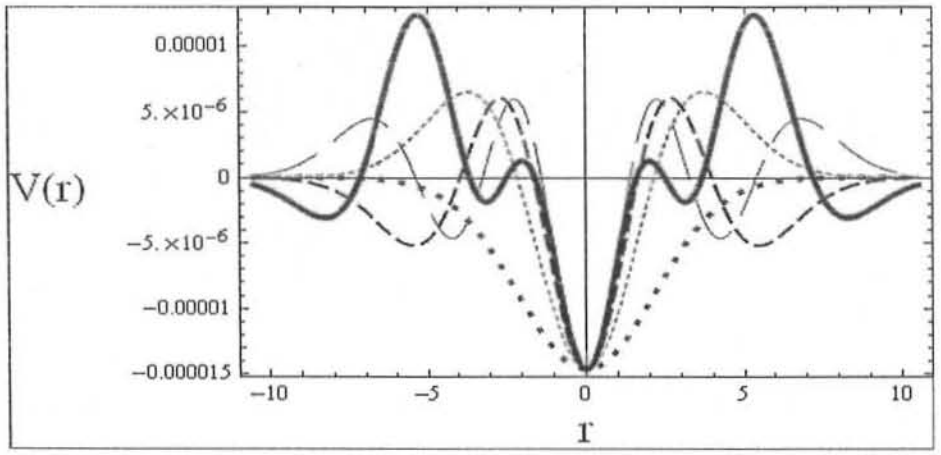

Figure 4-2: Shows the LG potential profiles for changing radial mode number $p = 0$ (square doted curve), $p = 1$ (small doted curve), $p = 2$ (small dashed curve), $p = 3$ (long dashed curve), $p = 4$ (solid curve) and with fixed $l = 0$, $\omega_0 = 3\lambda$, where $\lambda = 0.7149\ cm$.

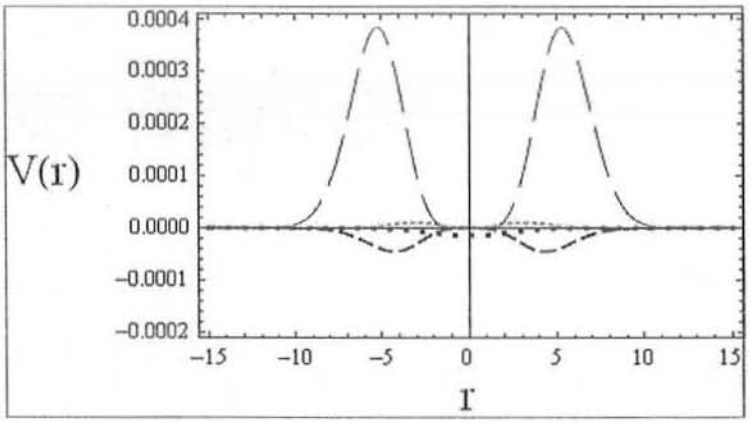

Figure 4-3: Shows the LG potential profiles for varying the angular mode number $l = 0$ (square doted curve), $l = 1$ (small doted curve), $l = 2$ (small dashed curve), $l = 3$ (long dashed curve), $l = 4$ (solid curve). with $p = 0$, $\omega_0 = 3\lambda$,and $\varphi = \pi$

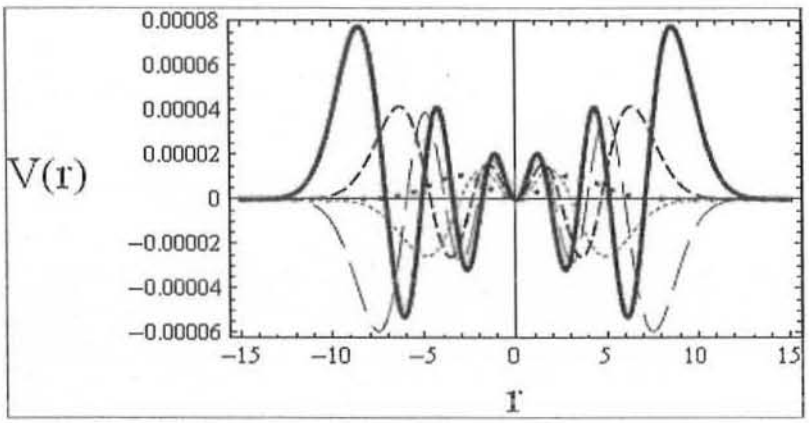

Figure 4-4: Shows the LG potential profiles involving EA waves for $p = 0$ (square doted curve) $p = 1$ (small doted curve), $p = 2$ (small dashed curve), $p = 3$ (long dashed pink curve), $p = 4$ (Solid curve). with fixed $l = 1$, $\omega_0 = 3\lambda$, and $\varphi = \pi$.

Bibliography

[1] Peter A. Sturrock, " An Introduction to the Theory of Astrophysical, Geophysical & Laboratory Plasmas" (Cambridge University Press, United Kingdom, 1994).

[2] R.D. Hazeltine, F.L. Waelbroeck. "The Framework of Plasma Physics" (Westview Press, America 2004).

[3] R. O. Dendy. "Plasma Dynamics" (Oxford University Press, United Kingdom 1990).

[4] Daniel Hastings, Henry Garrett. "Spacecraft-Environment Interactions" (Cambridge University Press, United Kingdom 2000).

[5] Irving Langmuir and Lewi Tonks, Phys. Rev. **34**, 876 (1929).

[6] I. P. Shkarofsky, T. W. Johnston, M. P. Bachynski, "The Particle Kinetics of Plasma", (Addison-Wesley Pub. Co., U.S.A.) 1966).

[7] M. Y. Tanaka, K. Nagaoka, A. Okamoto, S. Yoshimura, and M. Kono, IEEE Trans. on Plasma Sci. **33**, 454 (2005).

[8] M.Y. Tanaka, S. Yoshimura, IEEE Trans. on Plasma Sci. **36**,1224 (2008).

[9] K. Nagaoka, A. Okamoto, S. Yoshimura, M. Kono, and M. Y. Tanaka, Phys. Rev. Lett. **89**, 075 001.1 (2002).

[10] S. S. Harilal,1 T. Sizyuk, A. Hassanein, D. Campos, P. Hough, and V. Sizyuk. Applied Phys. **109**, 063306 (2011).

[11] Richard Fitzpatrick, "Brief History of Plasma" wikipedia 2011-03-31.

[12] Suresh Chandra "Textbook of Plasma Physics", (CBS Publishers and Distributers Pvt. Ltd, New Delhi, 2010).

[13] Jesse Russell and Ronald Cohn, "Van Allen Radiation Belt" (Book on Demand Press, Liverpool 2012).

[14] A.A. Gusev, G.I. Pugacheva, U.B. Jayanthi, and N. Schuch. Brazilian J. Phys. **33**, 775 (2003).

[15] S. R. Elkington, M. K. Hudson, A. A. Chan. "Enhanced Radial Diffusion of Outer Zone Electrons in an Asymmetric Geomagnetic Field". American Geophys. Uni. Spring Meeting 2001.

[16] Y. Y. Shprits and R. M. Thorne. Geophys. Research Lett. **31**, 8 (2004).

[17] Richard B. Horne, Richard M. Thorne. et al; Nature **437**, 227 (2005).

[18] Martin Walt, "Introduction to Geomagnetically Trapped Radiation" (Cambridge University Press, United Kingdom 1994).

[19] Y. I. Feldstein Geomagnetism and Aeronomy **3**, 183 (1963).

[20] Y. I. Feldstein, American Geophys. Uni. 67, 761 (1986).

[21] E. G. Gibson "The Quiet Sun; National Aeronautics and Space Administration", (Washington, D.C. USA 1973).

[22] Yukio Katsukawa and Saku Tsuneta. The Astrophys. J. **621**, 498 (2005).

[23] H. Alfvén, Nature, **150**, 405 (1942).

[24] T. Elfouhaily and D. R. Thompson, Geophys. Research J. **106**, 4655 (2001).

[25] K. Iwai, K. Shinya, K. Takashi, and R. Moreau, Magnetohydrodynamics **39**, 245 (2003).

[26] Albert Messiah "Quantum Mechanics" (Wiley, New York 1958.)

[27] L. Brillouin "Wave Propagation in Periodic Structures" (Dover Publications Inc. Mineola, New York 1946).

[28] Lighthill, James, "Waves in fluids", (Cambridge University Press, New York 1978).

[29] M. J. Lighthill "Group velocity", (Oxford University Press, Wellington United Kingdom (1997).

[30] W. D. Haye "Group velocity and nonlinear dispersive wave propagation", (Proceedings of the Royal Society of London, Series A, Math. and Phys. Sci. 1973)

[31] S. M. Barnett, and L. Allen, Optics Commun. **110**, 670 (1994).

[32] L. Allen, M. W. Beijersbergen, R. J. C. Spreeuw, and J. P. Woerdman, Phys. Rev. **45**, 8185 (1992).

[33] L. Allen, M. Padgett, and M. Babiker, Prog. Opt. **39**, 291 (1999).

[34] M. Harris, C.A. Hill, P.R. Tapster, and J.M. Vaughan, Phys. Rev. **49**, 3119 (1996).

[35] M.J. Padgett, J. Arlt, N.B. Simpson, and L. Allen, Am. J. Phys., **64**, 77 (1996).

[36] J. Leach, M.J. Padgett, S.M. Barnett, S. Franke-Arnold, and J. Courtial, Phys. Rev. Lett., **88**, 257901 (2002).

[37] Sharon A. Kennedy, Mallhew J. Szabo, Hllary Teslw, James Z. Porterfied, and E. R. I. Abraham. Phys. Rev. A **66**, 04380 (2002).

[38] G. A. Turnbull, D. A. Robertson, G. M. Smith, L. Allen, and M. J. Padgett, Opt. Commun. **127**, 183 (1996).

[39] R. A. Beth, Phys. Rev. **50**, 115 (1936);

[40] J. D. Jackson, Classical Electrodynamics, 2nd ed. (Wiley, New York, 1962).

[41] J. Schwinger, L. L. DeRaad, Jr. K. A. Milton, and W. Tsai, "Classical Electrodynamics" (Perseus Books Reading, Massachusetts, 1998).

[42] C. S. Liu and V. K. Tripathi, "Interaction of Electromagnetic Waves with Electron Beams and Plasmas" (World Scientific Publishing Co. Pvt. Ltd, Singapore,1994).

[43] C. Cohen-Tannoudji, J. Dupont-Roc, and G. Grynberg, "Photons and Atoms" (Wiley, New York, 1989).

[44] J. M. Jauch and F. Rohrlich, "The Theory of Photons and Electrons", 2nd ed. (Springer-Verlag, Berlin,1979).

[45] L. Allen, M. Babiker, and W. L. Power, "Azimuthal Dopper-shift in light-beams with orbital angular momentum," Opt. Commun. **112**, 141 (1994).

[46] J.T. Mendonca, B. Thide, and H. Then, Phys. Rev. Lett. **102**, 185005 (2009).

[47] W. Kruer, "The Physics of Laser Plasma Interactions", (Addison-Wesley publishing Company, Redwood 1973).

[48] J. Courtial, D. A. Robertson, K. Dholakia, L. Allen, and M. J. Padgett, Phys. Rev. Lett. **81**, 4828 (1998).

[49] J. Weber, Am. J. Phys. **22**, 618 (1954) ".

[50] G. Molina-Terriza, Phys. Rev. A **78**, 053819 (2008).

[51] F. Tamburini and D. Vicino, Phys. Rev. A **78**, 052116 (2008).

[52] J. T. Mendonica, S. Ali, and B. Thide, Phys. Plasmas **16**, 112103 (2009).

[53] N. B. Simpson, K. Dholakia, L. Allen, and M. J. Padgett, Opt. Lett. **22**, 52 (1997).

[54] M. Bandyopadhyay, A. Tanga, P. McNeely, and V. Yaroshenko, Plasma Phys. **44**, 624 (2004).

[55] A. E. Siegman, Lasers (University Science Books, New Jersey 1986).

[56] M. K. Ayub, S. Ali, and J. T. Medonica, Phys. Plasmas **18**, 1022117 (2011).

[57] L. Yin et al., Phys. Plasmas **15**, 013109 (2008).

[58] B. Bezzerides, D. W. Forslund, and E. L. Lindman, Phys. Fluids **21**, 2179 (1978).

[59] R.E. Ergun, Y.J. Su, L. Andersson, C.W. Carlson, J.P. McFadden, F.S. Mozer, D.L. Newman, M.V. Goldman, and R.J.Strangeway, Phys. Rev. Lett. **87**, 045003 (2001).